INSTRUMENTS AND METHODS OF INVESTIGATION PACS numbers: 07.55.Db, 41.20.Gz, 75.30.Gw, **75.50.–y**, 75.60.Ch, 81.40.Rs

Strong stray fields in systems of giant magnetic anisotropy magnets

V N Samofalov, D P Belozorov, A G Ravlik

DOI: 10.3367/UFNe.0183.201303e.0287

Contents

Abstract. This paper reviews research into a little-studied phenomenon in which strong stray fields arise in ferromagnets with giant magnetic anisotropy. Conditions for this to occur and for the fields to be stable are discussed. A classification of strong fields is presented. For different field types, limiting field strength values on approaching singular points are determined. Applications of the stray fields in various technical devices are considered.

V N Samofalov, A G Ravlik National Technical University 'Kharkiv Polytechnic Institute',
ul. Frunze 21, 61002 Kharkov, Ukraine
E-mail: samofalov@kpi.kharkov.ua
D P Belozorov National Science Center 'Kharkov Institute of Physics and Technology',
ul. Akademicheskaya 1, 61108 Kharkov, Ukraine

Received 9 July 2011, revised 24 July 2012
Uspekhi Fizicheskikh Nauk **183** (3) 287 – 306 (2013)
DOI: 10.3367/UFNr.0183.201303e.0287
Translated by S N Gorin; edited by A Radzig

1. Introduction

1.1 Strong stray field: what is that?

Since the 1980s, information has appeared in the literature concerning systems of permanent magnets that generate stray fields with a strength that significantly exceeds the magnitude of the saturation induction B_s of the material of the magnets [1–9]. Halbach [1, 2] substantiated the possibility of creating large stray fields using permanent magnets. Halbach's concepts underwent further development in Refs [3–9]. Thus, a system of magnets was designed in Grenoble, in which a field with strength $H \approx 50$ kOe was obtained in a narrow gap ($\Delta d \approx 0.15$ mm) [7]. Somewhat lower stray fields ($H \sim 35$ kOe) were achieved in a so-called Halbach cylinder but in a cavity with a larger diameter ($d \approx 6$ mm) [9]. In Refs [10–12], the concept of *a strong field* was introduced to characterize such large magnetic fields — *it is a stray field whose strength H exceeds the saturation induction B_s of the material of the magnet: $H > B_s = 4\pi M_s$.*

The properties of permanent magnets have been studied for quite a long time and, naturally, the question arises as to why strong fields have been discovered only recently, and why most work on the generation of strong fields using systems of permanent magnets and investigations of these systems were performed only in the last two–three decades? In the well-known monographs on magnetism [13–16], strong fields were not even mentioned at all. This situation can be explained as a consequence of a number of causes. One of the conditions for the practical realization of strong fields is the presence of permanent magnets with a giant magnetic anisotropy and large coercive force. The strong stray fields generated by conventional permanent magnets, e.g., those made of Al–Ni–Co alloys, barium ferrites, and other materials [13–16], could not be detected earlier because of the absence of giant magnetic anisotropy in them. Such magnets were designed only in the 1960s on the base of rare-earth metals (REMs).

Another cause, one that is by no means less important, was that the existence of strong stray fields had not been predicted previously and, therefore, they were not sought for purposefully. This cause being more likely conceptual in character has to do with the following. As is well known [15, 16], the sum of diagonal components of the tensor of the demagnetizing factor of a uniformly magnetized ellipsoidal body satisfies the equality $N_{xx} + N_{yy} + N_{zz} = 4\pi$. Hence, a groundless conclusion was drawn that the demagnetizing field cannot exceed the field $H = 4\pi M_s$ in magnitude. Such a field, as is well known [13, 14], arises in a narrow gap between flat permanent magnets that are coupled by a magnetic conductor, or in a narrow slot in a uniformly magnetized ferromagnet. However, this is invalid for bodies of a non-ellipsoidal shape with a nonuniform magnetization. In the last case, the tensor N_{ik} cannot be reduced to a diagonal form in all points of a body, and the off-diagonal components N_{xy}, N_{xz}, N_{yz} can be quite large. Such situations have merely not been considered, i.e., the possibility of the existence of strong fields was excluded *a priori*.

1.2 Permanent magnets with giant magnetic anisotropy

Notice that in all known systems generating strong fields, magnets made of REM-based alloys are employed. The properties of REM magnets were well studied up to the 1980–1990s [17–23]. The fact that in systems of magnets with giant magnetic anisotropy strong stray fields arise became known after issuing the publications [2–7]. Prior to describing in detail the specific features of strong stray fields, it is necessary to briefly characterize those properties of permanent magnets that have a direct bearing on the theme of this paper. We will predominantly consider the problems of large anisotropy, high coercive force H_c, and the magnetic energy W of the material of the magnets.

It is known [17] that the stray fields reach their highest values in permanent magnets when the magnets reside in the uniformly magnetized (single-domain) state. A single-domain state is a metastable state. An energetically more favorable state is a multidomain (demagnetized) state. In a partly demagnetized state, the magnet can become unsuitable for generating strong fields. The demagnetization occurs because of the action of self-demagnetizing fields $\mathbf{H}_d$, whose strength is defined as $\mathbf{H}_d = -N\mathbf{M}$, where N is the demagnetizing tensor. In general, the demagnetizing field has a component $H_{\parallel}$, which is collinear with the magnetization vector $\mathbf{M}_s$ and is directed opposite to it, and a component $H_{\perp}$ which is perpendicular to $\mathbf{M}_s$. The stray field component directed opposite to the vector $\mathbf{M}_s$ leads to the appearance of domains of reversed magnetization if the coercive force H_c (or the value of the magnetic field necessary for the formation of nuclei of magnetization reversal) of the magnet material is less than the demagnetizing field: $H_c < H_d$.

Table 1. Characteristics of some rare-earth intermetallic compounds utilized in the production of permanent magnets. Figures enclosed in square brackets indicate works from which these characteristics were borrowed (T_C is the Curie temperature).

Compound	H_K, kOe	M_s, G	H_c, kOe	$(BH)_{max}$, MG Oe	K_1, 10^6 erg cm^{-3}	T_C, K
$SmCo_5$	200–400 [24]	850 [24]	15–20 [25]	18–20 [26]	170 [24]	1003 [24]
$Nd_2Fe_{14}B$	100 [24]	1280 [24]	10–20 [25]	25–50 [25]	50 [24]	585 [24]
Sm_2Co_{17}	70 [24]	955 [24]	7,5–25 [26]	27–30 [26]	33 [24]	1190 [24]

Table 1 contains the basic characteristics of some materials for permanent magnets. It is seen that the magnets of commercial fabrication possess a coercive force $H_c = 10-20$ kOe. It should be noted that values of $H_c \approx 83$ kOe were reached in laboratory $SmCo_5$ samples, [17], while the appropriate values in FePt films prepared by deposition run into $H_c \approx 50$ kOe [27]. The values of H_c given in the table are lower than the theoretical limit for the irreversible rotation of magnetization, which, as is known, is equal to the field of uniaxial anisotropy $H_K = H_c = 2K_1/M_s$. Therefore, to obtain high values of H_c, the material of the magnet should have a large magnetic anisotropy. This is valid for the mechanisms of magnetization reversal by both the irreversible rotation of magnetization and the displacement of domain walls. The component $H_{\perp}$ of the demagnetizing field that is perpendicular to $\mathbf{M}_s$ gives rise to a rotation of the magnetization. If the anisotropy constant is not great, the magnetization vector will deflect from the easy axis (EA) by a significant angle; as a result, the magnet will be partially demagnetized.

So then to realize a uniformly magnetized state in a magnet and thereby to reach high values of magnetic energy, the material of the magnet should have large magnetic anisotropy.

Notice that the compounds of REMs with 3d metals have, predominantly, a hexagonal or a rhombohedral lattice. Because of the large difference in atomic radii of the REMs and transition metals Fe, Co, Ni, and Mn, such binary systems form intermetallic compounds in which the EA coincides with the symmetry axis of the crystal.

A characteristic feature of all materials presented in Table 1 is large uniaxial magnetic anisotropy with a constant $K_1 \sim 10^7-10^8$ erg cm^{-3} and anisotropy field $H_K = 2K_1/M_s \geqslant 10^5$ Oe. In the work of K P Belov and his disciples [18, 21], such anisotropy was called *giant*. The authors of Refs [18, 21] emphasize that for many REM materials the ratio W_a/W_{exch} of the anisotropy energy to the exchange energy ranges 0.05–0.50. For example, W_a/W_{exch} for $SmCo_5$ is approximately 0.25, and $W_a/W_{exch} \approx 0.35$ for Dy [21]. In our paper, we have chosen another parameter to characterize materials with large magnetic anisotropy, namely $Q = K_1/2\pi M_s^2$, which is known as a 'quality factor' [28]. The application of the Q factor permits one to more correctly determine the conditions necessary for the realization of strong fields. We assigned uniaxial ferromagnets with $Q \geqslant 10$ to materials with a giant magnetic anisotropy. Thus, magnets made of $SmCo_5$ with a quality factor $Q \sim 50$ are assigned to materials with giant anisotropy, whereas magnets made of the NdFeB compound with $Q \sim 10$ should be considered as referring to a transition range.

Let us now briefly formulate the concepts on the nature of anisotropy. At present, there is no common point of view concerning the origin of the anisotropy of REM materials. Two theories may be cited that explain the nature of large anisotropy in REM compounds. One of these, the *single-ion theory* [29], ascribes the large magnetic anisotropy to the interaction of 4f electrons with the crystal field of the lattice. The orbital moment of 4f electrons is not 'frozen' because of the screening by 5s electrons; therefore, the most favorable orientation of the total magnetic moment is specified by the electrostatic field of the lattice. The other theory explains the giant anisotropy in REM compounds by the *anisotropy of the indirect exchange* [30, 31]. Thus, we see that the mechanisms of the emergence of anisotropy in REM compounds and in 3d metals are different. The magnetic anisotropy of 3d metals is related to the spin–orbit interaction of d electrons [23, 32].

An important characteristic of permanent magnets is the maximum energy product $W = (HB)_{\max}$, the theoretical limit of which is $(HB)_{\max} = 4\pi^2 M_s^2$ [17]. However, the values of $(HB)_{\max}$ in real samples that are found from the parameters of hysteresis loops are always less than the theoretical limit.

The highest values of magnetic characteristics are inherent in the magnets that find themselves in a *uniformly* magnetized state. It should be noted that for the realization of such a state, the substance of the magnet should possess a giant magnetic anisotropy and large coercive force. As is shown in Section 2, such requirements for the substance of a magnet should also be fulfilled to obtain strong fields.

2. Possibility of the existence of strong stray fields as a consequence of the solution to some magnetostatic problems

2.1 Schlömann problem

If we turn to the history of the problem of strong stray fields, we find that the possibility of their existence was first noted by Joseph and Schlömann [33]. The authors of this work did not calculate stray fields above permanent magnets; therefore, their results have only an indirect relation to the theme of strong stray fields. In paper [33], only a stray field that arises above a ferromagnetic sample made of a magnetically soft material in the form of a parallelepiped placed in a strong external magnetic field with $H \sim 100$ kOe was studied. It has been shown that the strength of the stray field near an edge of the parallelepiped varies depending on the distance r according to a logarithmic law with exceptional (singular) points near the edge. The data on the stray fields obtained in Ref. [33] could also be assigned to permanent magnets of the same shape made of materials with large anisotropy. Indeed, the uniaxial magnetic anisotropy exerts an effect on the magnetic state of a ferromagnet, which is similar to the action of an external field. The authors of Ref. [33], which was published in 1965, apparently did not know of new REM-based materials for permanent magnets that appeared at that time. The results of the calculations could also be extended to the case of permanent magnets with a large uniaxial anisotropy. However, the possibility of generating strong stray fields above permanent magnets with a large anisotropy remained outside the field of observation of the authors of Ref. [33]. If the researchers of stray fields had turned earlier to paper [33], the strong fields could have been discovered already in the 1970s.

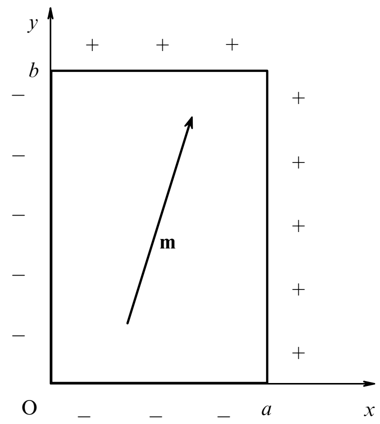

Figure 1. Calculation of stray fields arising near an edge of a uniformly magnetized parallelepiped: **m** is the unit vector indicating the direction of magnetization in the magnet.

2.2 Thiaville problem

In the later study [34], which was performed in 1998, Thiaville and colleagues substantiated the fundamental possibility of the existence of strong stray fields by analyzing stray fields arising near a single permanent magnet in the form of a parallelepiped. The authors of Ref. [34] performed a calculation and analysis of stray fields generated at an edge of a uniformly magnetized magnet (Fig. 1). They showed that the H_x component near a corner point O is described by the following dependence

$$H_x = M_s m_y \ln \frac{(a-x)^2 + y^2}{x^2 + y^2}, \tag{1}$$

where a is the dimension of the magnet along the x-axis, and $\mathbf{m}_y$ is the unit vector parallel to the y-axis.

It follows from expression (1) that the component H_x of the stray field at small distances $r = (x^2 + y^2)^{1/2}$ from the edges of the parallelepiped reaches values exceeding B_s. Upon approaching point O, the strength of the magnetic field, according to Eqn (1), tends to infinity by a logarithmic law, and the points at the edge of the parallelepiped are singular. Thus, the authors of Ref. [34] showed that the main previously unknown feature of stray fields is *the existence of a singularity*.

Since this singularity is related to uniform magnetization, the authors of Ref. [34] determined the degree of the possible deviation of the magnetization from the EA near the edge of the magnet, assuming that the existence of a large tangential component of a stray field should lead to a deflection of the magnetization vector from the initial direction $\mathbf{m}_0$ by δm_x, δm_y. The solution of the variational problem has shown that $\delta m_x \approx 0$ and $\delta m_y \approx 0$. This means that a large tangential stray field does not lead to a deflection of the magnetization from the initial direction even near the edge of the parallelepiped, where the stray field tends to infinity. A uniformly magnetized state is also retained at the edge of the magnet near the singular points.

The authors of Ref. [34] explained this unexpected result by the fact that, at the edge of the magnet, both the stray field and the exchange field tend to infinity. The directions of these fields are mutually opposite and they compensate for each other. Hence, the distribution of the magnetization even at the edge of the magnet should remain homogeneous. This conclusion requires a more detailed analysis. The point is that the exchange field becomes comparable in magnitude with the stray field at distances x that are less than the interatomic spacing. In addition, there are no physical grounds for increasing the exchange field. Therefore, it is doubtful that a large demagnetizing field near the edge of the magnet does not lead to a deflection of the magnetization from the EA. The actual distribution of the magnetization in materials with large but finite values of the field of the uniaxial anisotropy will hardly be strictly homogeneous. The appearance of a magnetization inhomogeneity will lead to a decrease in the strength of the stray field near the edge of the magnet. However, the singularity in this case is retained. Therefore, the data on the distribution of magnetization in the vicinity of singular points of a magnet is of fundamental importance.

In the work of Rave et al. [35] published in the same year as that of Thiaville et al. [34], a singularity in a corner point of the magnet shown in Fig. 1 is also discussed. The authors of Ref. [35] expressed opinion that the stray field according to the continuum theory of micromagnetism diverges logarithmically in the *mathematically* ideal corner of a magnetic body. Note that a similar logarithmic dependence also takes place in exactly solvable model problems. This singularity also arises in the case of the continuum theory of micromagnetism considered in Ref. [36]. This confirms the qualitative correctness of the results obtained by the magnetostatics method which, indeed, has a big advantage when considering complex systems.

Based on a numerical solution of micromagnetic problems, stray fields have been calculated near a corner of a magnet. Thus, a numerical calculation of stray fields was performed in Ref. [35] with an increasing number of computed points, and it was shown that these fields stop increasing at distances of order $l = \sqrt{A/K_d}$ (where A is the exchange constant, and K_d is a constant that characterizes the stray field energy). This characteristic length l for all known materials significantly exceeds interatomic distances; therefore, the effects related to the atomic lattice can be neglected in the micromagnetic approach.

Thus, these two studies [34, 35] supplement each other. These studies for the first time considered the problem of singularity emergence and pointed to the ways of solving this problem, but they gave no answer to the question of what the magnitude of the stray fields near the edge of the magnet is (see Fig. 1). To resolve this problem, one should apparently depart from the macroscopic approach to the calculations of the field and, in addition, it is important to obtain experimental data on the magnitude of the field in the vicinity of the singular point.

2.3 Kittel problem

The possibility of the existence of strong magnetic fields also follows from the solutions to other magnetostatics tasks, which do not relate directly to permanent magnets, e.g., from the calculation of the models of a domain structure. Thus, Kittel [37, 38], when determining equilibrium parameters in the model of an open domain structure (see inset to Fig. 2), used the so-called method of magnetic charges. The dimension of the plate (and of domains) in the direction of the y-axis was assumed to be infinite. In Refs [37, 38], stray fields were not considered; therefore, formulas directly describing the strength of stray fields above the domains are absent. The authors of Refs [11, 12] determined the dependence of the strength of stray fields above the domains in the Kittel structure using an expression for the potential of the magnetic field of a stripe domain structure given in Ref. [39].

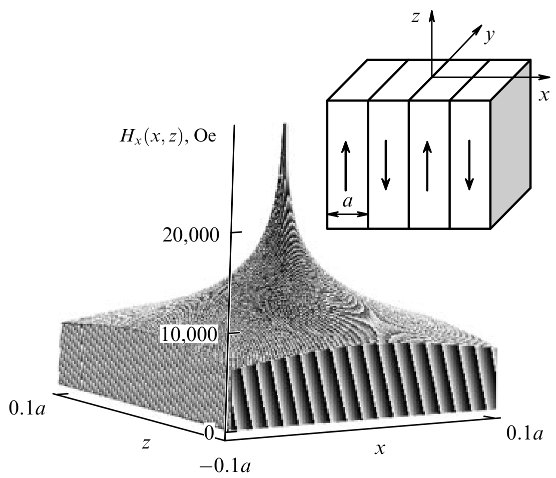

Figure 2. Dependence of the $H_x(x, z)$ component of the stray field in the model of an open Kittel domain structure shown in the inset. In the calculations, the value of M_s was assumed to be 700 G.

After calculating the gradient of the potential, we found in Ref. [11] the $H_x(x, z)$, $H_z(x, z)$, and $H_y(x, z)$ dependences for the stray field components. Because of the symmetry, the stray field component $H_y(x, z) = 0$, and the vertical component $H_z(x, z)$ is relatively small: $H_z(x, z) < 2\pi M_s$. The stray field component $H_x(x, z)$ above the domains is characterized by the following dependence

$$H_x(x, z) = 8M_s \sum_{n=0}^{\infty} \frac{1}{2n+1} \cos \frac{(2n+1)\pi x}{a} \times \exp\left(-\left|\frac{(2n+1)\pi z}{a}\right|\right). \qquad (2)$$

It should be noticed that the field $H_x(x, z)$ in formula (2) is only determined by the system of charges on the upper face of the plate. The lower face was assumed to be removed to infinity. It is seen from formula (2) that H_x at the points $x = na$ and $z = 0$ tends to infinity and, in the vicinity of these points in a range of width $\Delta x \approx a/10$, it takes on values that exceed the magnitude of the induction of the ferromagnet material, i.e., $H_x > 4\pi M_s$. The specific features of the stray-field component $H_x(x, z)$ in the vicinity of the point O for the region $-0.1 < \Delta x/a < 0.1$, $-0.1 < \Delta z/a < 0.1$ manifest themselves clearly in the dependence demonstrated in Fig. 2, from which it is seen that the stray-field component H_x reaches high values.

2.4 Strong stray fields in films with stripe domains

Ch Kittel carried out his analysis in 1948, when film materials with large magnetic anisotropy were not yet known. Such materials appeared only in the 1960s, when iron–garnet films with a perpendicular anisotropy were discovered. For many of these films, the quality factor is $Q > 10$, which ensured the appearance of an open stripe domain structure in them. The calculation of stray fields above the walls of stripe domains in an open one-dimensional model was performed by Schlömann in Refs [40, 41]. The dependence obtained by Schlömann for the tangential component H_t of the stray field above a domain is written down as $H_t(z) = H_x(z) = 2M \ln\left[(c+z)/(c-z)\right]$, where $2c$ is the film thickness. It follows from this dependence that, on the film surface ($z = c$) above the middle part of the domain wall, the field increases infinitely. Schlömann [40, 41] indicates that the stray fields lead to a change in the wall energy, but the singularity in the exceptional point has not been discussed in detail in these studies.

A similar expression for the stray field above a Bloch wall of stripe domains was obtained by Slonczewski [42]: $H_t(z) = H_y(z) = 4M \ln\left[z/(h-z)\right]$. This dependence is valid at the film thicknesses h exceeding the width δ_0 of the domain wall. As is seen, the field component H_t tends to infinity on the film surface ($z = h$). According to Slonczewski [42], this field leads to a 'twisting' of the magnetization near the film surface; i.e., the magnetization vector goes out of the wall plane and the wall cannot now be considered as a Bloch wall. It should be noted that, according to Eqn (2), a large demagnetizing field arises also in a stripe domain near its wall. This field can lead to a deflection of the magnetization vector from the EA in a local region of the domain if, e.g., Q factor is small. In our opinion, the magnetization twisting in the domain structure can be neglected for $Q > 10$. It should be noted that the appearance of large stray fields above stripe domains of an open structure is confirmed by the results of recently performed calculations [43, 44]. Additionally, in some work (in particular, in Ref. [45]) logarithmic dependences for materials with $Q \leqslant 1$ similar to expression (2) were given for the H_t field.

In the 1970–1980s, a number of theoretical studies appeared [46–49], in which the calculations were performed in terms of open one-dimensional models for a stripe domain structure in thin films with a moderate perpendicular anisotropy $H_K \leqslant 4\pi M_s$ ($Q < 1$). The authors of these studies did not calculate stray fields above stripe domains. Meanwhile, the computation of stray fields could indicate the instability in such fields of a one-dimensional stripe domain structure in ferromagnets with small anisotropy. Indeed, the appearance of a large demagnetizing field in materials with $Q < 1$ should lead to a deflection of the $\mathbf{M}_s$ vectors in the domains from the easy axis toward the field direction. As a result, the distribution of the magnetization in the domains should become inhomogeneous. Numerous discussions concerning this problem terminated in the late 1990s with the advent of papers [50, 51], in which, on the basis of numerical calculations in terms of micromagnetic models, an inhomogeneous distribution (over the layer thickness) of the magnetization in stripe domains was established. Earlier, this was revealed experimentally in Refs [52–56].

2.5 Calculations of stray fields in a system of two magnets

The presence of large stray fields directly above the stripe domains in an open Kittel structure can hardly be checked using ordinary experimental methods because of the small width of the domains and, consequently, a narrow region of localization of the strong field. The authors of Ref. [11] suggested using, for such a check, a system of two magnets magnetized similarly to two neighboring domains in an open Kittel structure. According to expression (2), strong stray fields should arise at the surface near the interface of the domains. Such a simple system of magnets, which was called in Ref. [11] an A type system (Fig. 3a), consists of two permanent magnets in which the magnetization vectors have mutually opposite directions, and of a magnetic conductor. The calculations and the analysis of stray fields for this simple system of magnets permit one to clarify the nature and specific features of strong fields.

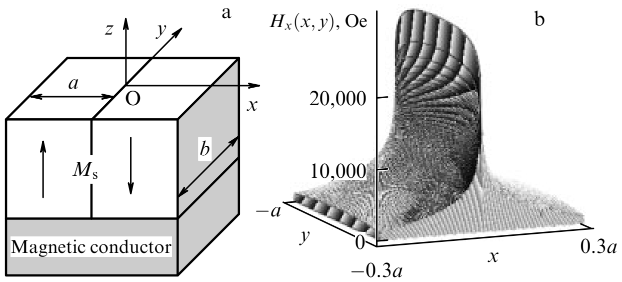

Figure 3. (a) Schematic of the system of two magnets with a magnetic conductor — system A. (b) Strength of the stray field component $H_x(x, y)$ for the points located on the plane xy ($z = 0$). When constructing this dependence, it was assumed that $b = 2a$ and $M_s = 1000$ G.

For these calculations, we employed the method of 'magnetic charges'. According, for instance, to Ref. [57], the stray field established by the magnetization $\mathbf{M}$ is written out as

$$\mathbf{H}(\mathbf{r}) = -\mathrm{grad}\,\varphi(\mathbf{r}), \tag{3}$$

where $\varphi(\mathbf{r})$ is the magnetostatic potential

$$\varphi(\mathbf{r}) = -\int_V \frac{\mathrm{div}\left(\mathbf{M}(r')\right)\mathrm{d}\mathbf{r}'}{|\mathbf{r}-\mathbf{r}'|} + \int_S \frac{\mathbf{M}_i(r')\,\mathrm{d}\mathbf{S}_i}{|\mathbf{r}-\mathbf{r}'|}, \tag{4}$$

$\mathrm{d}\mathbf{r}' \equiv \mathrm{d}x'\,\mathrm{d}y'\,\mathrm{d}z'$, V is the volume of the ferromagnet, $\mathbf{M}_i(r')$ is the ith component of the magnetization vector, and $\mathrm{d}\mathbf{S}_i$ is the ith component of the vector $\mathrm{d}\mathbf{S}$. The magnetostatic field H meets the boundary conditions for the continuity of the tangential component of the field and for the normal component of the induction:

$$\mathrm{rot}\,\mathbf{H}(\mathbf{r}) = 0, \qquad \mathrm{div}\,\mathbf{B} = \mathrm{div}\,(\mathbf{H} + 4\pi\mathbf{M}) = 0. \tag{5}$$

It follows from the second equation in Eqn (5) that in a ferromagnet, where $\mathrm{div}\,\mathbf{M} \neq 0$, surface or volume magnetic charges arise with a density $\sigma = -\mathrm{div}\,\mathbf{M}$. The first integral in formula (4) takes into account the contribution from volume charges, while the second integral takes into account the contribution from surface charges. Using formulas (4) and (5), we can calculate the strength of the stray field if the densities of surface (σ_s) and volume (σ_m) charges are known.

The authors of Refs [11, 12] assumed, when calculating the system A, that the distribution of the magnetization over the volume of the magnet is homogeneous. This condition is acceptable if the maximum value of the horizontal component H_x of the stray field is significantly smaller than the uniaxial anisotropy field H_K of the magnet material. In this case, we have $\sigma_v = 0$, and the surface charges with a density $\sigma_s = \pm M_s$ will arise on the upper faces that are parallel to the plane xy. It was assumed that $\sigma_s = 0$ on the surfaces of magnets that contact the magnetic conductor. For the last condition to be fulfilled, special magnetic conductors are required. The point is that a magnetic conductor made of a magnetically soft material with a very large permeability will not ensure the complete closure of the magnetic flux. Problems related to the optimization of magnetic conductors for a system A and other systems of magnets require independent consideration.

The distribution for the vertical component H_z of the stray fields is written out as

$$H_z(x,z) = 2M_s\left(\arctan\frac{a+x}{z} - \arctan\frac{a-x}{z} - 2\arctan\frac{x}{z}\right). \tag{6}$$

It follows from last formula that the stray field $H_z(x,z)$ at all points above the magnets of the system is relatively small: $H_z(x,z) \leqslant 2\pi M_s$. The field component $H_z(x,z)$ makes a small contribution to the total field $H = (H_x^2 + H_z^2)^{1/2}$.

The stray fields component $H_x(x,z)$ for $b \gg a$ (Fig. 3a) is written out as

$$H_x(x,z) = M_s\big[\ln(a^2+z^2+2ax+x^2) - 2\ln(x^2+z^2) + \ln(a^2+z^2-2ax+x^2)\big]. \tag{7}$$

In the case of small $x < 0.01a$ and $z = 0$, dependence (7) takes on a simple form: $H_x(x) \approx 4M_s \ln(a/x)$. For the points on the z-axis, the dependence is analogous, i.e., $H_x(z) \approx 4M_s \ln(a/z)$. It also follows from formula (7) that when approaching point O along any direction, the field $H_x(x,z)$ increases equally monotonically according to a logarithmic law $H_x(x) \approx 4M_s \ln(a/r)$, reaching large values. If $b \sim a$, the expressions for the tangential component $H_x(x,y)$ of the stray field is awkward and, therefore, is not given here. This component is shown graphically in Fig. 3b, from which it is seen that the strongest field arises on the surface of magnets near the boundary between them, and that the field remains strong along the entire boundary length.

It is seen from the results of the calculations that the strength of the stray fields can substantially exceed the saturation induction value of the magnet, $H_x > B_s = 4\pi M_s$. Because of the continuity of the tangential component of the stray field, the same field will be inside the magnet, as well, i.e., the demagnetizing field H_d will also be large. Using the definition of the demagnetizing field $\mathbf{H} = -N\mathbf{M}_s$ [58] and formulas (6) and (7), we can find all components of the tensor N for system A. For points located near the plane xz of the magnets ($z \approx 0$), the tensor component $N_{xz} = 4\ln(x/a)$ and, as is seen, can take on large values. Thus, strong stray fields arise in bodies of a nonellipsoidal shape, and they are caused by large values of the off-diagonal components of the tensor of the demagnetizing factor.

Thus, the emergence of strong stray fields in system A is related to a uniformly or almost uniformly magnetized state of the magnet. Using Eqns (5)–(7), we can determine the conditions of the stability of a uniformly magnetized state. From condition (5) maintaining the continuity of the tangential component of the demagnetizing field, it follows that the demagnetizing field inside the magnet (for $z \leqslant 0$) and for small $x < 0.01a$ is characterized by the following dependence: $H_x(x) \approx 4M_s \ln(a/x)$. At a small distance $r = (x^2+z^2)^{1/2}$ from the y-axis, the field strength reaches values of $H > B_s$. This large demagnetizing field is directed perpendicular to the easy axis, and in materials with a reduced value of H_K can lead to a significant deflection of the magnetization vector from the EA at points of the magnet that lie close to the y-axis. Therefore, a necessary condition for the existence of large fields is the fulfillment of the requirement $H_x^{\max} < H_K$. In addition, it follows from Eqn (6) that the vertical component H_z of the demagnetizing field reaches a maximum in the center of the magnet of system A and that $H_z \leqslant 2\pi M_s$. At the center of the magnet, the H_z component of the demagnetizing field is directed opposite to the magnetization vector. If the coercive force of the magnet material is $H_c \leqslant 2\pi M_s$, domains arise with a reversed magnetization, i.e., a partial demagnetizing will occur. If the above-mentioned conditions $H_x^{\max} < H_K$ and $H_c > 2\pi M_s$ are not fulfilled, Eqns (6) and (7) cannot be used for the calculation of the field strengths. Therefore, it is fundamentally important also to determine the minimum value of the $H_K/H_x^{\max}$ ratio above which magnetization 'twisting' near singular points can be neglected. The evaluation of these limiting values is of large scientific and practical importance.

To estimate the $H_K/H_x^{\max}$ ratio, calculations for an isolated magnet in the shape of a parallelepiped have been performed. It was assumed that the magnet is a crystal with a primitive cubic lattice with a lattice parameter a, in each site of which resides an atom with a magnetic moment μ equal to the Bohr magneton: $\mu = \mu_B = 10^{-20}$ erg G^{-1}. The dimension of the magnet along the y-axis was assumed to be infinite. In this case, the magnetization lies in the plane xz and its orientation on each site of the cubic lattice is specified by a single angle $\theta_{i,k}(x,z)$. The equilibrium direction of the magnetic moments $\boldsymbol{\mu}$ on each site of the cubic lattice is determined from the condition of the minimum of free energy, including the anisotropy energy, the exchange energy and the magnetic field energy. The parameter to be calculated is the angle $\theta_{\max}$ at points on the edge of the magnet.

The results of calculation of $\theta_{\max}$ at various values of the field H_K of uniaxial anisotropy and of the field H_x are presented in Table 2. The adopted values of the field strength approximately correspond to the values of the limiting demagnetizing field generated by a single isolated magnet, by a system of two magnets, and by some complex system (such as a Halbach cylinder).

As is seen from Table 2, the maximum angle of deflection $\theta_{\max}$ of the vector $\boldsymbol{\mu}$ from the EA does not exceed 10° at large values of the uniaxial anisotropy constant ($K > 10^8$ erg cm^{-3}, $H_K > 200$ kOe). At the angle $\theta_{\max} = 10°$, the charge density near a singular point is $\sigma \approx 0.985 M_s$, which is lower (by less than 2%) than the limiting value of the charge density in the case of a strictly uniform magnetization ($\sigma = M_s$). It should be emphasized that the actual value of $\theta_{\max}$ will be somewhat

Table 2. Results of calculations of the maximum angle of magnetization twisting, $\theta_{\max}$, for permanent magnets at different values of the anisotropy field H_K and demagnetizing field H_x.

H_K, kOe	20	100	140	160	180	200	240	280	320	360	400
$\theta_{\max}$, grad ($H_x = 80$ kOe)	> 45	22.0	16.0	14.00	12.00	11.50	9.50	8.2	7.20	6.40	5.80
$\theta_{\max}$, grad ($H_x = 50$ kOe)	> 45	13.7	10.1	8.90	7.90	7.18	6.01	5.1	4.50	4.00	3.60
$\theta_{\max}$, grad ($H_x = 35$ kOe)	> 45	9.6	7.1	6.26	5.57	5.00	4.20	3.6	3.17	2.82	2.54

lower, since the adopted values of the field $H_x = 35$, 50, and 80 kOe for the systems under consideration are overestimated, whereas the value of the exchange constant $A_a = 10^{-14}$ erg per atom is underestimated.

Thus, it follows from the estimates performed that in an isolated magnet and in a system of two magnets with a large anisotropy the magnetization twisting near singular points can be neglected if the maximum value H_{max} of the demagnetizing field does not exceed $0.3H_K$. At equal values of M_s, the magnitude of the limiting field in the system of magnets made of $SmCo_5$ should be higher than that in the system of magnets made of Nd−Fe−B alloys. The anisotropy fields in these systems are 400 and 80 kOe, respectively. It is also seen from Table 2 that the angle θ_{max} cannot exceed 10° in magnets with $H_K < 80$ kOe and magnetization $M_s \sim 1000$ G. In this case, the magnetization distribution cannot be assumed to be uniform, and more exact calculations of the stray field strengths should be carried out to determine the limiting magnetic field.

It follows from the relationship $H_x(x) \approx 4M_s \ln(a/x)$ that as $x \to 0$ the tangential component H_x of the stray field tends to infinity. Since the stray field, in view of various physical factors, cannot be arbitrarily large, the question arises of the true magnitude of the field at the singular point and in its small vicinity. It seems to be impossible to find an answer to this question within a macroscopic approach. This problem can be solved within a theory that takes into account the atomic structure of ferromagnets. The need for the development of such a theory is obvious, since the laws of a continuum cannot be extended to a discrete medium without the appearance of contradictions. This theory should also specify the applicability boundary of the macroscopic approach.

3. Experimental proof of the existence of strong fields

3.1 Measurement of stray fields in a system of two magnets

Thus, the possibility of generating strong magnetic fields by permanent magnets has been substantiated theoretically. The aim of further investigations is to experimentally check the existence of strong stray fields and of the logarithmic dependence of the field strength H_t on distance from the gap between the magnets. To this end, we used in Ref. [11] a system of two $SmCo_5$-based magnets (Fig. 3a) with dimensions of 40 × 40 × 20 mm each. The schematic of measurements with the use of film sensors is given in the inset to Fig. 4. The magnitude H of the fields was measured by magnetoresistive sensors made on the base of granulated Ag−Co films. These sensors, which had the form of narrow rectangular strips (3 mm long, 0.1 mm wide, 0.1 μm thick), possessed a giant magnetoresistive effect, with $\Delta R/R = 20-25\%$, and became saturated in a magnetic field $H \sim 25$ kOe [59].

During the measurements, the plane of the sensor was parallel to the plane yz (see inset to Fig. 4). The distance from the sensor to the y-axis was varied using plates of various thicknesses. The sensor was placed near the origin of system A. In Fig. 4, the black circles denote the measured strengths of the stray field. It is seen that there is good agreement between the experimental values of the field and the calculated results obtained with the logarithmic dependence $H_x(x) \approx 4M_s \ln(a/x)$.

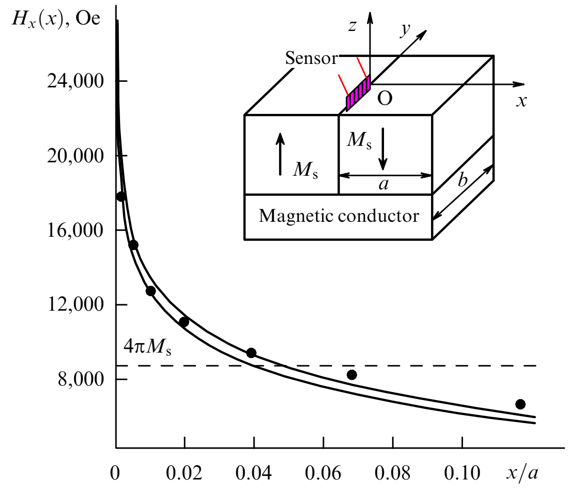

Figure 4. Comparison of the experimental strengths of a stray field above a system of two magnets with the calculated dependences $H_x(x) = 3000 \ln(a/x)$ and $H_x(x) = 2700 \ln(a/x)$. The measurement scheme for the stray fields above the system of two magnets is shown in the inset.

Additional proof of the existence of strong stray fields above the magnets of system A is given by the data of investigations performed with the aid of an electron paramagnetic resonance (EPR) spectrometer [60, 61]. The source of a dc magnetic field in the EPR device is also a system of two $SmCo_5$ magnets (Fig. 3a). The control sample of an amorphous $Fe_{40}Ni_{40}B_{20}$ alloy made in the form of a narrow strip of a thin tape with dimensions of 15 × 15 μm was mounted on a quartz plate. The sample was placed near the maximum of the static magnetic field and in the maximum of the magnetic component of the resonant electromagnetic field. The resonance absorption was detected at a frequency of 44 GHz. It has been shown that for the frequency $\nu_{res} = 44$ GHz the static magnetic field near the gap with allowance made for the effect of the demagnetizing field reached a value of $H_{res} \approx 19$ kOe. These experiments also convincingly confirm the existence of strong stray fields.

Magnetooptical investigations of strong stray fields using iron garnet films made it possible to obtain information not only on the strength of the field but also on its configuration; i.e., this method enables the researcher to visualize the field above the magnets. In Ref. [62], iron garnet films with a large field of perpendicular magnetic anisotropy ($H_K \approx 8$ kOe) served as indicating medium. It has been established that the pattern of regions with stripe domains, which arises in the indicator at its various distances from the magnets, corresponds to the calculated lines of equal strength for this system. Figure 5 displays the domain structure near the edge of the boundary between the magnets. The strength of the strong fields was evaluated from the values of the limiting distance z_{cr} from the magnet plane at which the labyrinthine domain structure disappeared.

Thus, the presence of strong stray fields in system A has been proved experimentally using three different methods.

4. Limiting values of strong fields

4.1 Classification of strong fields

Thus, the possibility of the existence of strong magnetic stray fields has been substantiated theoretically and proved

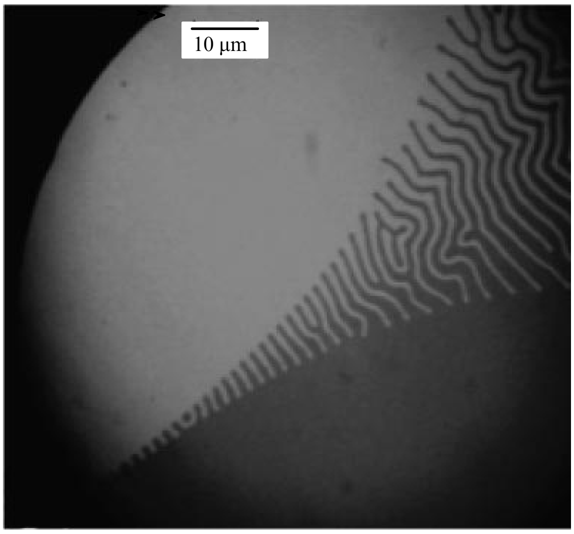

Figure 5. Domain structure in an iron garnet film near the edge of the boundary between the magnets of a system A at $t = 280$ μm.

experimentally through the example of a simple system of two magnets. Good agreement between the calculated and measured strengths of the fields generated by a system of magnets made of $SmCo_5$ has been observed. This indicates that the employment of the method of magnetic charges is justified for the calculations of stray fields in magnets with large values of the H_K field. The application of this method makes it possible to obtain analytical expressions for the field strength and then reveal the specific features of strong fields.

In paper [63], we called the largest stray field, which can be reached in a given system of magnets at admissible dimensions of the magnets and reasonable values of their magnetic parameters, a *limiting* stray field. For characterizing strong stray fields, we introduced in paper [63] the following parameters: $H_{\max}$ is the maximum value of the stray field, Δr is the size of the region of localization of the strong stray field, $|\nabla H_{\max}|$ is the limiting magnitude of the gradient of the field, and $\langle H \rangle$ is the average value of the stray field in some volume near the system of magnets. The introduction of these parameters makes it possible to compare various systems that generate strong fields and to carry out their classification.

The problem on the calculation of limiting values of strong fields is reduced, on the whole, to the determination of such a geometry of magnets and such a distribution of the magnetization in them, which provide the strongest stray fields near *singular points* of a given system of magnets. In general, this variational problem has not yet been solved. A solution was found for a particular problem concerning uniformly magnetized magnets with magnetic charges on their surfaces. Notice that all possible types of magnets can be divided into two types according to the type of the magnetic state, namely, those with *uniform* and *nonuniform* magnetizations. In practice, systems consisting of magnets with a uniform magnetization are predominantly used. In such systems, the strong fields are caused by magnetic charges that arise on their surfaces.

A charged surface can be both flat and curved. As a result of the solution of a variational problem, it has been shown in paper [64] that in uniformly magnetized magnets the largest stray field arises at a rectilinear edge of a plane, i.e., *a strong field is an edge phenomenon*. Therefore, below, when calculating limiting fields, we will predominantly consider magnets in the form of parallelepipeds and right-angle prisms.

It can be assumed, *a priori*, that various types of systems of permanent magnets exist, which have a capacity for generating strong magnetic stray fields. Depending on the type of the region of localization of strong fields, we divided them in paper [63] into three types: *linear, point, and uniform*. A characteristic feature of *linear fields* is the fact that the singular points lie on some line. Usually, an edge of the magnet serves as such a directional line. The region of the localization of a strong linear field represents a cylinder of radius Δr, whose axis is this directional line. An example of a linear field may be a stray field that arises along the perimeter of the faces of the parallelepiped or near the directrix of a right cylinder uniformly magnetized along its axis. In the latter case, the region of localization represents a torus. Thus, the field inside a Halbach cylinder [2] is defined as a combination of linear fields, and it can also be considered linear.

The strong magnetic stray fields that arise, for example, near the vertex of a uniformly magnetized cone or a pyramid, or at the line of intersection of charged planes of magnets and are localized in some closed vicinity of a singular point, were called *point* fields [63]. The linear and point fields can also arise in magnets with a *nonuniform* magnetization (see Section 6).

A characteristic feature of strong *uniform stray fields* is that they are independent of edge effects. These fields have a large region of localization. Systems of magnets in which the strong field represents a combination of fields of the above three types are also possible.

4.2 Limiting values of linear fields. Open systems

The aim of the investigations that were performed in paper [63] was to find such a geometry of a system of magnets and such directions of magnetization in this system, which could allow obtaining the largest values of fields near singular points. This is of high importance for both the physics of magnetic phenomena and for practical applications. It is hardly possible to solve such a problem using only numerical methods. Therefore, it is important to find analytical dependences for the field strength. Since the solution to a variational problem for the calculation of a limiting field in the general case of arbitrary magnetizations is absent, in papers [63, 64] we assumed, when finding limiting dependences for the above three types of strong fields, that the magnets are uniformly magnetized. This solution to the variational problem narrows the circle of searching for the desired systems: only bodies having faces in the form of *flat surfaces* are considered.

Systems that induce strong magnetic stray fields can consist of one or several magnets. By changing the configuration of a system, the dimensions and shapes of the magnets, their number in the system, and also the orientation of the magnetization in them, we can affect the limiting magnitudes of the generated strong fields. In paper [63], the extremum of the field strength $H(\varphi_i, \alpha_i)$ was determined as a function of the vertex angles α_i of the prism and of the direction angles φ_i of the magnetization.

It has been found that the strongest field is generated by a single magnet having the shape of a *right parallelepiped*. This field arises at the middle of the edge of the magnet and its magnitude is independent of the direction of the magnetization vector. The field strength is calculated from the dependence $H \approx 2M_s \ln(a/r)$, where r is the distance to the

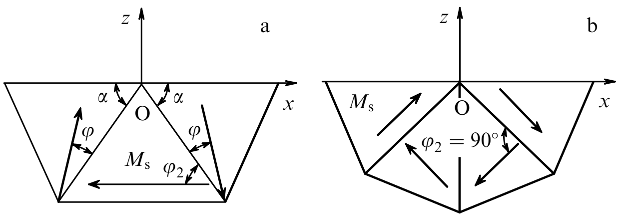

Figure 6. Open systems consisting of (a) three, and (b) four magnets in the form of right prisms.

edge, $r = (x^2 + z^2)^{1/2}$. It should be noted that this dependence gives somewhat overestimated values of the field, since the true dependence for $b \gg a$ is as follows: $H = M_s \ln [1 + (a/r)^2 - 2ax/r^2]$. However, the overestimation is small for $r \ll a$; therefore, the limiting field can be calculated using the above expression $H \approx 2M_s \ln (a/r)$. The terms discarded from the true expression for the field strength H predominantly affect the region Δr of the strong field localization. This approach makes it possible to compare various systems of magnets generating strong fields, since the field strength will be characterized only by the prelogarithmic coefficient $A(n)$.

It should be noticed that in the case of a single magnet, shown in Fig. 1, the strong demagnetizing field near some vertices of the parallelepiped is co-directional with the vector $\mathbf{M}_s$, whereas near two other vertices it is directed opposite to this vector. This means that the demagnetizing fields can both stabilize the magnetic state in some regions of the magnet and destabilize it in other regions. All these circumstances should be taken into account when constructing a system of magnets generating strong fields.

In a system of two magnets, the strongest field arises near the edges of magnets that have the shape of right parallelepipeds (y-axis in Fig. 3). In this case, the magnetization vectors in the neighboring magnets should be oriented in mutually opposite directions and should lie in the plane xz. The strength of the limiting field is calculated from the dependence $H_x \approx 4M_s \ln (a/r)$ if the dimensions of the magnets along the y-axis are much greater than those along the x-axis ($b \gg a$).

In the system displayed in Fig. 6, the strong stray field is concentrated above the outer xy surface of magnets (half-space $z > 0$). Such systems are called *open*. In an open system of three or four magnets, the strong fields will be largest at the points located near the y-axis, i.e., in the region of contact of the edges of the trihedral prisms. It has been found that the limiting fields for systems of three and four magnets are characterized by the dependences $H_{max} \approx 3\sqrt{3}M_s \ln (a/r)$ and $H_{max} \approx 4\sqrt{2}M_s \ln (a/r)$, respectively. For an optimized system of three magnets, such a dependence is realized at the angles $\varphi = 0$, $\varphi_2 = 60°$, and $\alpha = 60°$. For a system of four magnets, the field will be largest at the angles $\varphi = 0$, $\varphi_2 = 90°$, and $\alpha = 45°$.

4.3 Strong stray fields in closed systems of magnets. Halbach cylinder

If we connect symmetrically to the plane xy that is optimum for a system of two magnets (Fig. 3a) a similar system in such a manner that the vectors $\mathbf{M}_s$ in neighboring magnets are oriented in mutually opposite directions, then the stray field for the points located in the vicinity of the y-axis will double [will reach $H_{max} \approx 8M_s \ln (a/r)$]. Since the strong field is localized in a narrow cavity near the y-axis of the system surrounded by four magnets, such a system was called *closed* (Fig. 7). In the cavity of the closed system, the magnetic field will be smaller than follows from the above dependence $H_{max} \approx 8M_s \ln (a/r)$. Such a system of four magnets with an internal cavity is equivalent to two systems A with a slot whose charged planes are turned relative to one another by an angle of 90°. The system with a slot shown in the inset to Fig. 8 was called a system B. The strong fields are retained also in the presence of a gap with a width of 2δ between the flat surfaces of the magnet (see Fig. 8). The strength of the horizontal component of the magnetic field is described by the expres-

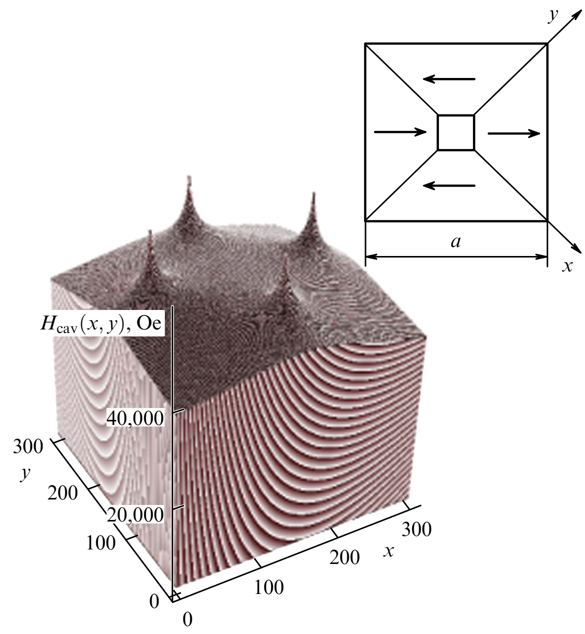

Figure 7. Strength of the stray field component $H_{cav}(x, y) = (H_x^2 + H_y^2)^{1/2}$ constructed for the region $-0.015a < x < 0.015a$, $-0.015a < y < 0.015a$ for a closed system consisting of four magnets in a Halbach cylinder (see inset); the dimension of the square cavity along the diagonal is equal to $2\delta = 0.02a$.

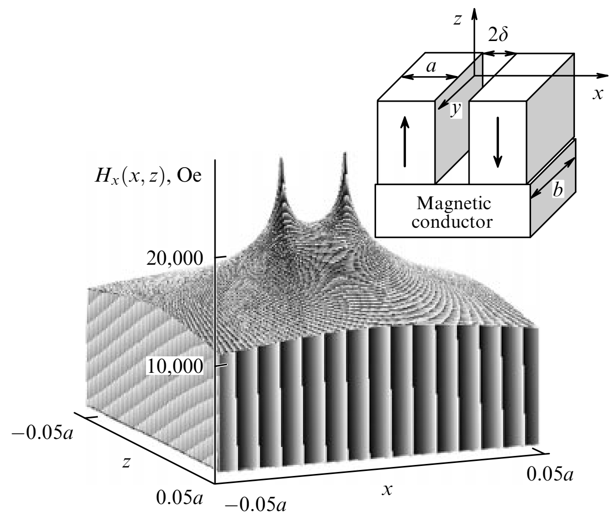

Figure 8. Strength of the stray field component $H_x(x, z)$ in a system of two magnets with a gap (see inset). When constructing this dependence, it was assumed that $b = 2a$, $M_s = 1000$ G, and $2\delta = 0.01a$.

sion

$$H_x(x,z)=M_s\Big\{\ln\big[(a+\delta+x)^2+z^2\big]+\ln\big[(a+\delta-x)^2+z^2\big] - \ln\big[(\delta+x)^2+z^2\big]-\ln\big[(\delta-x)^2+z^2\big]\Big\}. \qquad (8)$$

As is seen from Fig. 8, the singular points, at which the field tends to infinity, appear in the $H_x(x,z)$ dependence; they are located at the edges of the gap with coordinates $z=0$ and $x=\pm\delta$.

The system shown in the inset to Fig. 7 serves, in fact, as the simplest Halbach cylinder. Thus, the field in the cavity of this cylinder is equal to the geometrical sum of the fields that are generated by two B type systems and of the field produced by charges located on the cavity faces. For the points lying near the center of the cavity, the field is characterized by the following dependence: $H_{\mathrm{cav}}(x,y)=(H_x^2+H_y^2)^{1/2}$. Figure 7 illustrates the $H_{\mathrm{cav}}(x,y)$ dependence inside the cavity. When constructing this dependence, the contribution from the charges on the surface of the cavity, just as that from the outer surface of the system, has not been taken into account.

As Fig. 7 suggests, the magnetic field inside the cylinder has high values and is nonuniform. The sharp peaks visible in the figure indicate the presence of four singular points. These points belong to the edges of charged faces. Therefore, the field in such a cavity is nonuniform. Notice that the field will also be nonuniform in the cavity of a Halbach cylinder and other similar systems. It can be assumed that the limiting field in a closed system of six and eight magnets is two times higher than that in open systems of three and four magnets (see Fig. 6). Therefore, we can use the respective dependences $H_{\max}(r)\approx 6\sqrt{3}M_s\ln(a/r)$ and $H_{\max}(r)\approx 8\sqrt{2}M_s\ln(a/r)$, when calculating the limiting field in the cavities of systems with six and eight magnets. Upon increasing the number of pairs of magnets, the field strength in the cavity also increases. A comprehensive answer has been given in Ref. [63] to the question of what the form of the limiting $H_{\max}(r)$ dependence in the cavity of a closed system will be. Here, we briefly report the general principles that were used for constructing such a system.

It has been shown that a complex system of magnets represents a combination of elementary systems. When constructing an optimum system, the simplest elements were used. In paper [63], we chose as the simplest element a system of magnets similar to system A (quadrupole), i.e., a pair of unlikely charged faces lying in the same plane and having a common rectilinear boundary. Such a system can be realized utilizing magnets in the form of trihedral prisms (sectors). The vertices of the prisms should be located at a minimum distance from a certain axis.

The field strength in a narrow gap between the pairs of faces is $H_t\approx H_x\approx 4(\pm\sigma)\ln(a/r)$, where $\pm\sigma$ are the densities of charges on neighboring faces. The magnetic field generated by one pair can be strengthened by adding other similar pairs to this pair. Then, the total field near the boundary will be equal to the geometrical sum of the fields generated by each simple element. The field in a cylinder consisting of $4n$ sectors ($n=1,2,\ldots$) in the form of triangular prisms was calculated. The stray field strength for the component H_x after the implementation of algebraic transformations under the sign of the sum is expressed as follows:

$$H_x(n)=8M_s\ln\frac{R}{r}\,n\sin\frac{\pi}{2n}\,. \qquad (9)$$

Using the last formula, we can calculate the magnetic field inside a Halbach cylinder with a very small inner diameter at an arbitrary number of sectors, as well as estimate the magnitude of the maximum achievable field H_x for the case where the number of magnets in the system tends to infinity. Thus, it follows from formula (9) that the strength of the limiting field is given by

$$\lim_{n\to\infty}H_x(n)=H_{\max}=4\pi M_s\ln\frac{R}{r}\,. \qquad (10)$$

Expression (10) shows that, when increasing the number of magnets to infinity, the limiting value of the coefficient $A(n)$ is equal to 4π. The values of the coefficient $A(n)$ that characterizes the field strength $H_x(n)=A(n)M_s\ln(R/r)$ in the Halbach cylinder are given in Table 3.

Table 3. Values of the prelogarithmic coefficient $A(n)$ for closed systems with the number of magnets n.

n	4	6	8	10	14	16	20
$A(n)$	8.00	10.30	11.20	11.70	12.15	12.24	12.36

Thus, the limiting value of the linear field in systems of magnets with a uniform magnetization cannot exceed a value that is determined by the relation $H=4\pi M_s\ln(R/r)$. In real systems with a finite number of magnets n, the field strength will always be somewhat lower because of the dispersion of easy axes in the magnet and twisting of magnetization vectors near singular points. Therefore, the limiting field strength should be determined from the expression $H_{\max}=B_r\ln(R/r)$, where B_r is the remanence.

In 1985, Halbach [2] suggested a system of magnets consisting of sectors in the form of right prisms. This system, which is shown schematically in the inset to Fig. 9, is called a Halbach cylinder. Each sector here is magnetized uniformly. The magnetization vector in each sector lies in the plane that is perpendicular to the cylinder axis. The

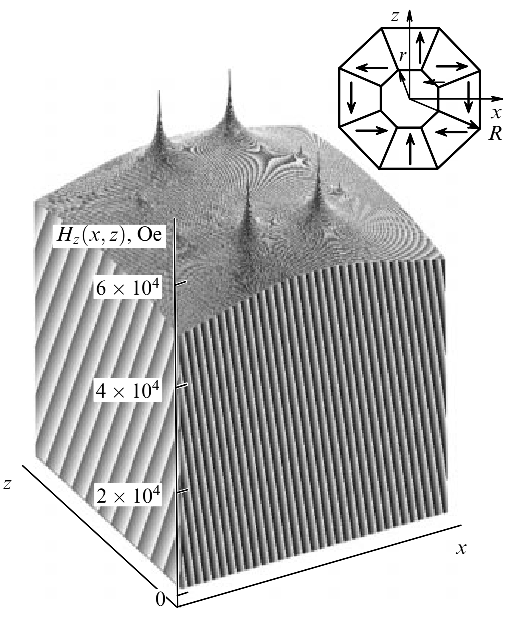

Figure 9. Strength of the stray field component $H_z(x,z)$ in a Halbach cylinder (see inset) constructed for the region $-0.015a<x<0.015a$, $-0.015a<z<0.015a$. In the inset, a Halbach cylinder consisting of eight magnets is shown in the section by the plane xz.

magnetization directions in the sectors are indicated in the figure by arrows. The strong field is generated in the cavity of the cylinder.

Halbach [2] calculated the stray fields arising in the cavity of such a cylinder, assuming that the cylinder height is much greater than its diameter ($L \gg r$). He calculated only the stray field component H_z (see Fig. 9). The two other components in the center of a long cylinder ($L \gg r$) were assumed to be significantly less than H_z.

It follows from the dependence ($H_z \approx B_r \ln(R/r)$) given in paper [2] that the strength of the field component H_z in the cylinder cavity is constant. This is emphasized by the author himself, and by the authors of Refs [3, 4]. However, the statement about the uniformity of the stray field in the cavity of the cylinder is unjustified. Even with a qualitative consideration (see Fig. 9) it seems impossible that a uniform stray field can exist in the cavity of the cylinder near the edges of four pairs of 'charged' faces between the secors, i.e., in the case of four systems B.

Using a numerical solution to the variational problem, Zhakov [65] sought for a distribution of magnetization in a magnet that corresponded to a maximum stray field. It was shown that the stray field can exceed the saturation induction (i.e., can be strong) in the case of a magnetization distribution similar to the distribution of $\mathbf{M}_s$ in a Halbach cylinder.

5. Point sources of strong magnetic stray fields

Thus, the limiting value of a *linear* field is limited by the relationship $H = 4\pi M_s \ln(R/r)$. To find analogous limiting dependences for the *point field*, the authors of Refs [63, 66] have analyzed three types of point fields with the purpose of clarifying the possibility of obtaining dependences with a prelogarithmic coefficient $A(n) > 4\pi$ in other systems of permanent magnets, also.

5.1 Lines of intersection of charged planes as sources of a point field

If two or several intersecting charged surfaces are found in a system of magnets, then the field will reach a maximum magnitude at the points of intersection of the edges of these surfaces. In the inset to Fig. 10, such a system is shown, consisting of four identical magnets having the shape of sectors that are parts of a cylinder of radius R. The surface magnetic charges arise on the plane boundary of sectors matching, where $\operatorname{div} \mathbf{M}_s \neq 0$. These charges generate a strong field H_z.

Problems related to the limiting field of such systems were studied in Refs [63, 66]. It was shown that the strong field H_z will be largest when the magnetization vector in each magnet is directed along the bisectrix of the sector angle. In this case, the charge density on both planes is $\sigma_{xz} = \sigma_{yz} = \sqrt{2} M_s$. The strong field H_z in this system represents the sum of two linear fields and reaches maximum values at the singular point O. If we neglect the dependence of the field H_z on the charges arising on the external surface of the cylinder, the strength of the strong field in the vicinity of point O will be written out as

$$H_z \approx 4\sqrt{2} M_s \ln \frac{h}{r}, \tag{11}$$

where $r \approx (x^2 + y^2 + z^2)^{1/2}$ is the distance from point O to the point at which the field strength is measured, and h is the height. The $H_z(x, y)$ dependence at $z = 0$ is displayed in Fig. 10.

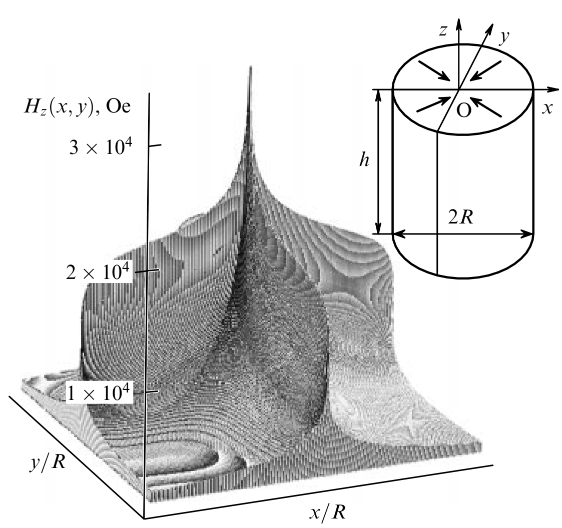

Figure 10. Strength of the stray field component $H_z(x, y)$ on the surface ($z = 0$) of a source of a point field, constructed for the region $-R < x < R$, $-R < y < R$. In the calculations, M_s was assumed to be equal to 1000 G. The source of the point field consisting of four magnets is depicted in the inset.

For a system consisting of n sectors, the field strength fits the dependence

$$H_z \approx 2n M_s \sin \frac{\pi}{n} \ln \frac{h}{r}. \tag{12}$$

When the number of sectors tends to infinity ($n \to \infty$), the limiting field near point O is defined by the expression

$$H_z = H_{\max} \approx 2\pi M_s \ln \frac{h}{r}. \tag{13}$$

It is obvious that all values of the field calculated via formulas (11)–(13) can be increased twofold if above the cylinder (see Fig. 10) we place a second similar cylinder. In this case, the magnetization vector should be directed in each sector of the second cylinder along its bisectrix from the center. The largest field in this case is characterized by the following dependence:

$$H_z = H_{\max} \approx 4\pi M_s \ln \frac{h}{r}. \tag{14}$$

An analysis of the dependence $H_z(x, y) = H_{\max}$ at $z = 0.01R$ revealed that the region of the strong field occupies almost half the area of the gap, i.e., $\Delta r \approx R$.

It follows from formula (14) that the limiting fields in a Halbach cylinder and at the above-considered point source are described by a similar dependence. The advantage of a point source is that in all the points of the system the strong field H_z inside the magnet (the demagnetizing field) is perpendicular to the magnetization vector, i.e., to the EA of the magnets. Such a mutual arrangement of the EA and H_z decreases the possibility of demagnetization of the magnets by their strong self-field. Therefore, such systems can be exploited for the production of record-high stray fields generated by permanent magnets.

5.2 Conical sources of point fields

Another type of source of strong point fields can be magnets in the form of a cone, pyramid, or spatial figures formed by a surface of revolution. Since the limiting values of their fields differ only insignificantly, the authors of paper [63] restricted themselves to an analysis of the systems of conical magnets. It

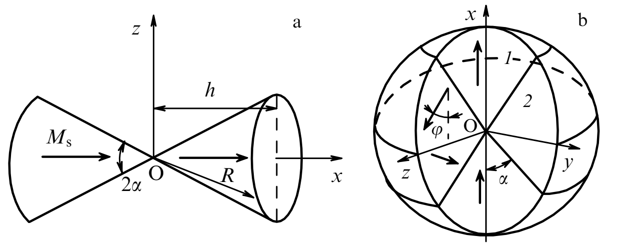

Figure 11. (a) System consisting of a pair of conical magnets. (b) System of two pairs of conical magnets separated by radial planes.

can easily be shown that the strong field generated by a right cone with a symmetrical section (under the assumption that the cone is uniformly magnetized along its axis) will be concentrated near the cone vertex, and the x-component of the field (Fig. 11) will be parallel to the symmetry axis. This strong field reaches a maximum value when the generatrix of the cone is a straight line. This follows from the solution of the variational problem when the surface of the cone is formed by the rotation of some curve $y(x)$ around the axis. If the magnetization vector $\mathbf{M}_s$ is parallel to the cone axis (x-axis), the density of charges on the conical surface is written out as $\sigma = M_s(y')/(1+y'^2)^{1/2}$, where y' is the derivative of $y(x)$. The magnitude of the axial component H_x of the field depends on the shape of the $y(x)$ curve that connects the cone vertex O with an arbitrary point at its lateral surface; near the cone vertex O, it is defined as follows:

$$H_x(x, y, y') = 2\pi M_s \int_0^x \frac{x y y'}{\left[(x+\delta)^2 + y^2\right]^{3/2}}\, dx\,, \qquad (15)$$

where δ is the distance to the observation point lying in the plane $x = -\delta$. Since the field reaches the limiting value in the vicinity of point O, the magnitude of δ should be very small, and in the first approximation we can neglect it and consider the point field lying only in the plane $x = 0$. The extrema of the functional (15) are determined by the solution to the Euler equation, which has the form

$$y = \pm\sqrt{2}x\,. \qquad (16)$$

Thus, the field in conical magnets reaches the greatest value near the cone vertex in that case, when the generatrix of the cone is a straight line: $y = \pm\sqrt{2}x$. The cone vertex angle is $2\alpha \approx 110°$. The strength of the axial component of the stray field for such a cone is defined as $H_{max} \approx 2.4 M_s \ln(h/r)$. In a system of two conical magnets arranged along the same axis (Fig. 11a), the magnetic field strength will be two times greater: $H_{max} \approx 4.8 M_s \ln(R/r)$.

It has been shown [63] that the highest fields are generated in more complex systems consisting of several pairs of cones (Fig. 11b). Two magnets of type *1* have the shape of cones, while the magnets of type *2* have the shape of hemispheres with a cut in the form of a cone. Both pairs of magnets form a sphere. The sphere is divided by radial planes into four sectors. The magnetization vector in each sector is parallel to the plane of the bisectrix of the dihedral angle and makes an angle φ with the axis of the cone (Fig. 11b). The entire system is placed into a special clip which holds the magnets from dispersion. In addition, it was assumed that this clip prevents the formation of charges on the external surface of the sphere. In such a combined system of magnets, the contribution to the stray field comes from the charges arising on both the conical surfaces and at the plane boundaries between the sectors.

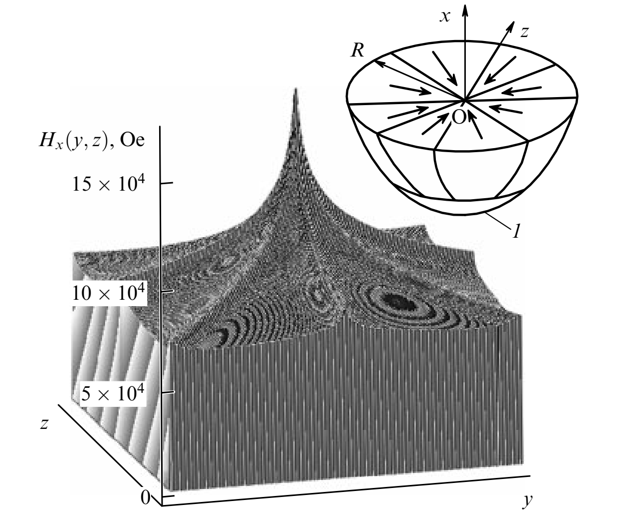

Figure 12. Strength of the field component $H_x(y, z)$ in the system shown in the inset for the region $-0.1R < z < 0.1R$, $-0.1R < y < 0.1R$. In calculations, M_s was assumed to be equal to 1000 G. The inset displays half of a system consisting of two pairs of conical magnets. The magnets of the system lying between the conical magnets *1* are separated by radial planes into eight sectors each.

Using the extremum condition for a function of several variables, optimum values of the desired angles were found, and then the limiting stray fields were calculated for the systems consisting of various numbers of pairs of conical magnets. Each pair of cones [except for the central one (see inset to Fig. 12)] was divided into eight equal sectors. Thus, for a system of two pairs of conical magnets, the numerical calculation evidenced that the field H_x will be largest at the angles $\varphi = 108°$ and $\alpha = 36°$. The limiting field dependence for these values of the angles takes the following form $H_x \approx 14 M_s \ln(R/r)$. Thus, we found $A(n) = 14$, which is more than 4π; consequently, this conical system of magnets generates a stronger field than does the linear one.

The calculated value of $A(n)$ (and of the field strength H_x) for a system of two pairs of conical magnets can be increased by addressing a similar system of three pairs of cones in such a manner that the pair of internal cones *1* remains uniformly magnetized in parallel to the cone axis, while the two external cones (cones of type *2* in Fig. 11b) are divided into eight sectors each. The calculation of such a system revealed that the coefficient $A(n)$ increases to $A(n) = 16$ at the following optimum values of the angles: $\alpha_1 = 24°$, $\alpha_2 = 62°$, $\alpha_3 = \pi/2 - \alpha_1 - \alpha_2$, $\varphi_1 = 0$, $\varphi_2 = 70°$, and $\varphi_3 = 139°$. It should be noticed that α_1, α_2, and α_3 are the cone vertex angles, and φ_1, φ_2, and φ_3 are the angles between the vector $\mathbf{M}_s$ and the cone axis. In a system of five pairs of cones, the limiting field near the vertex is given by the dependence $H_x \approx 17 M_s \ln(R/r)$. If the system consists of seven pairs of cones, the limiting field will assume the form $H_x \approx 18 M_s \ln(R/r)$.

Figure 12 depicts the dependence of the field $H_x(y, z)$, constructed for a system of two pairs of conical magnets shown in the inset to this figure. Each pair is divided here into eight sectors. Figure 12 reflects the specific features of the stray field in the gap between the hemispheres depicted in the inset. As is seen, the stray field near point O can become very strong: $H_x(y, z) \approx 10^5$ Oe at $R/r = 1000$. The point field in

Fig. 12 represents the sum of fields of two types: a field generated by conical sources, and fields arising at the line of intersection of charged planes.

One of the advantages of a conical system of magnets consists in the fact that the axial component of the demagnetizing field near the cone vertex is directed parallel to the vector $\mathbf{M}_s$ and, thereby, it stabilizes the uniformly magnetized state. This makes it possible to consider the conical systems of magnets being most suitable for obtaining record-high values of stray fields. The calculated estimates indicate the possibility of achieving, in a gap of width $0.001R$, field strengths ranging $H_x \approx 70-100$ kOe. Such values of the stray field appear to be limiting for all possible systems.

6. Strong stray fields in systems of magnets with a nonuniform magnetization

The possibility of the existence of strong stray fields in magnets with a *nonuniform* magnetization was theoretically substantiated in Refs [68, 69]. In such magnets there arise volume magnetic charges with a density σ_v, apart from surface charges with a density σ_s.

6.1 Cylindrical magnet

The inset to Fig. 13 depicts a magnet in the form of a cylinder in which the magnetization vector $\mathbf{M}_s$ has the same magnitude and is directed along the radius at each point. It was supposed that the radial distribution of the magnetization in this magnet is due to its radial texture in which the EA is directed along the radius of the cylinder, and the field of uniaxial anisotropy H_K of the magnet material is so large that the emerging stray fields do not virtually change the radial distribution of the magnetization in the magnet.

In the case of a radial direction of the magnetization in a cylindrical magnet (see Fig. 13), apart from surface magnetic charges with a density $\sigma_s = \pm M_s$, volume charges with a density $\sigma_v = \pm M_s/r$ also arise. As is seen, a specific feature of such a magnet is the presence of a high density of volume charges near the axis of the cylinder. Notice that although the density of volume charges increases upon approaching the cylinder axis, the charge in a volume of unit height $dv = 2\pi r\,dr$ remains finite, while the magnetization at the axis is uncertain. Magnets were considered with a cylindrical cavity of small radius r_0, in which $\sigma_v = 0$ and $\sigma_s = \pm M_s$. Just as in the preceding cases, the contribution from the charges located on the external surface was neglected. The influence of the charges can be minimized using special magnetic conductors built around permanent magnets.

The dependence of the field component $H_z(r, z)$ has a complex shape; it can be represented in a form suitable for an analysis only at the points lying on the z-axis. If we take into account only the contribution of volume charges, the field component H_z on the axis of a cylinder of infinite length for $r_0 \to 0$ is expressed as follows:

$$\lim_{r_0 \to 0} H_z = 2\pi M_s \ln \frac{2R}{z} \,. \tag{17}$$

If above the magnet depicted in Fig. 13 we place iniaxially a second identical magnet but with a different direction of magnetization, the limiting field will strengthen twofold, i.e., it will be defined as $H_z \approx 4\pi M_s \ln(2R/z)$. Thus, the limiting dependence for the point field of a cylindrical magnet with a radial magnetization has the same form as that for a linear field.

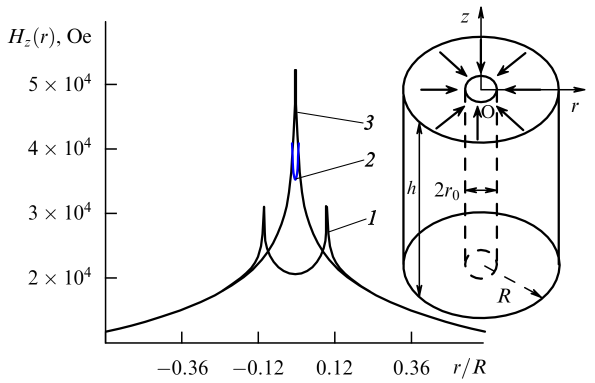

Figure 13. Strength of the stray field $H_z(r)$ for points lying on the endface ($z = 0$) of a cylindrical magnet at different dimensions of its cavity: (*1*) $r_0 = 0.1R$, (*2*) $0.01R$, and (*3*) $0.001R$. The inset displays a scheme of the magnet with a radial distribution of the magnetization.

Notice that the authors of Ref. [70] also calculated the stray fields above a hollow cylinder in two magnetic states: (1) with a radial magnetization, and (2) with a uniform magnetization parallel to the cylinder axis. The analytical expressions obtained for the strength of the stray field have a complex form and the existence of strong fields does not follow explicitly from them, in contrast to formula (17).

The $H_z(r)$ dependence has a more complex form than $H_z(z)$; therefore, peculiarities of the former can only be judged from the data given in Fig. 13 which shows the field components calculated from $H_z(r) = H_{zv}(r) + H_{zs}(r)$ at $z = 0$ and different values of the radius of the cylindrical cavity: $r_0 = 0.1R$, $r_0 = 0.01R$, and $r_0 = 0.001R$. To simplify the expressions, the height of the cylinder in the calculations was assumed to be infinite. A distinctive feature of the stray field of a magnet with radial magnetization, as is seen from Fig. 13, is the presence of a large region of localization of the strong field, which is comparable with the dimensions of the magnet: $\Delta r \approx R/2$. In the narrow gap of a system of two such magnets located uniaxially, the radius of the region of localization of the strong field is comparable with the diameter of the cylinder, i.e., the stray field strength is higher than the induction of the magnet material at almost all points of the region between the magnets.

To quantitatively characterize the inhomogeneous field in a gap of volume V between the magnets, the authors of Ref. [69] introduced an integral characteristic — an *average field* $\langle H \rangle$. The magnitude of the average field in the gap between the magnets was calculated as

$$\langle H \rangle = \frac{\int_V |H(x, y, z)|\,dV}{V} \,. \tag{18}$$

Notice that the magnitude of $\langle H \rangle$ makes it possible to compare different systems of magnets with one another. The average values of the field component $\langle H_z \rangle$ at different values of the gap width δ between two cylindrical magnets are given in Table 4, from which it is seen that the average value of the field, even in a wide gap between two magnets ($\delta \approx 0.1R$), is almost 1.8 times greater than $4\pi M_s$. The value of $\langle H_z \rangle \approx 23 M_s$ corresponds to the limiting achievable (at $\delta = 0$) average value of the field in the gap of this system.

Table 4. Calculated average values $\langle H_z \rangle$ of the field H_z.

Radius of the circular region of averaging the field H_z	R	R	R	R	$0.5R$	$0.5R$	$0.5R$
Relative distance δ between the magnets	0	$0.01R$	$0.1R$	$0.2R$	0	$0.01R$	$0.1R$
$\langle H_z \rangle$ values	$22.5M_s$	$22.4M_s$	$21M_s$	$20M_s$	$32M_s$	$31M_s$	$30M_s$

Thus, at $M_s = 1000$ G we obtain a field $\langle H_z \rangle = 23{,}000$ Oe. At $\delta = 0.1R$, the value of $\langle H_z \rangle$ becomes smaller, but remains sufficiently large. If, when calculating the average field, we also take into account the contribution from the radial component $H_r(r)$, the average values of the total field $\langle H \rangle = (H_z^2 + H_r^2)^{1/2}$ will only slightly exceed the values given in Table 4.

In a magnet having the shape of a hemisphere with a radial direction of the $\mathbf{M}_s$ vectors, the density of the volume charges in the hemisphere, $\sigma_v = \pm 2M_s/r$, is two times higher than that in the above-considered cylinder. The limiting values of the stray fields in magnets with a radial magnetization, however, do not exceed the magnitudes of strong fields in a cylindrical magnet with radial magnetization.

6.2 Quasinonuniform systems of magnets

A system of magnets in the form of sectors uniformly magnetized along the bisectrix of the dihedral angle in a cylinder with radial magnetization (see inset to Fig. 10), as well as other similar systems, were called in Ref. [68] *quasinonuniform*. The similarity between these systems and a magnet in the form of a cylinder with radial magnetization is not only external. It also manifests itself in a similar dependence of their volume density of charges $\sigma_v \sim M_s/r$ on the distance r to the center of the cylinder, and in the closeness of the values of the parameters for the strong field. In the system displayed in Fig. 10 there are no volume charges. Surface charges arise on neighboring faces between the sectors with a density $\sigma_s = 2M_s \sin(\pi/4)$ [or $\sigma_s = 2M_s \sin(\pi/8)$], forming a field of charges. The charges are distributed over the volume nonuniformly. The charged faces converge near the cylinder axis; therefore, the density of charges per unit volume increases, and such a field of charges can also be characterized qualitatively (apart from the surface density σ_s) by the charge density averaged over the volume, $\langle \sigma \rangle$. Thus, we have an average value of $\langle \sigma \rangle \approx 0.94M_s/r$ for a system of four magnets, and $\langle \sigma \rangle \approx 0.97M_s/r$ for a system of eight magnets, which differs only a little from σ_v of a magnet with radial magnetization. If the number of magnets in the system is large, then $\sigma_v = \langle \sigma \rangle \approx M_s/r$. As is seen, the volume average of the density of charges in a system of magnets is the same as in a magnet with radial magnetization.

As was noted above, the similarity between these systems and a magnet in the form of a cylinder with radial magnetization manifests itself, furthermore, in the close values of the strong field parameters. Thus, for points lying near the cylinder axis, the strengths of the limiting field of the H_z component for a quasinonuniform system with a large number of magnets and for a magnet with radial magnetization are characterized by the identical dependence $H_z(r) \approx 2\pi M_s \ln(h/r)$. Quasinonuniform systems, just as systems with radial magnetization, possess a large region of localization of the strong field [68].

6.3 Systems of magnets generating strong uniform fields

In all the systems described in Sections 4.2, 4.3, 5.1, 5.2, 6.1, and 6.2, the strong stray fields are related to the effects arising at the edges of charged planes. These systems of magnets are characterized by a large degree of nonuniformity of the strong field. As was shown in Ref. [68], the systems of magnets similar to the above-considered ones are not the only ones that can generate strong fields. A system of magnets of another type was studied in Ref. [68], which generates a field with a strength $H > 4\pi M_s$ over almost the entire width of the gap between flat surfaces of magnets. This field is close to uniform one throughout the gap.

In contrast to linear and point fields, the uniform strong field is characterized by the absence of singular points in the $H_z(x)$ dependence. A distinctive feature of a uniform strong field is that it is caused by the H_z component of the stray field, which is normal to the charged surface, rather than by the tangential component, as in the systems that were described above. In the narrow gap of a system of four magnets [68] with a magnetic conductor, the strength of the normal component of the field is 22% greater than the saturation induction, i.e., $H_z \approx 1.22B_s$. With increasing the number of magnets in the system, the field strength in its gap will also increase. For a system consisting of a large number of magnets, the limiting stray field reaches $\sim 1.5B_s$.

Concluding the discussion of the systems of magnets generating strong stray fields, it should be noticed that such fields also arise in ferromagnets placed in a magnetizing field of high strength. This was shown not only in Ref. [70], but also in Ref. [71], where an increase in a strong magnetic field H_h produced by an electromagnet was reached due to the use of conical concentrators made of materials with a high induction. At present, conical pole pieces made of Ho, Gd, and Dy are employed for the production of large fields in superconducting magnets [72, 73]. Notice that when considering such systems in the presence of an external source generating a field of strength H_h, it is expedient to extend the definition of the strong field given in Section 1.1. A field whose strength is $H > 4\pi M_s + H_h$ rather than $H > 4\pi M_s$, as in the case of permanent magnets, should be called a *strong field*. This type of strong magnetic field is not considered in this paper.

7. Gradient of strong fields

A distinctive feature of most systems of magnets considered above lies also in the fact that the stray fields in them are both large in magnitude and strongly nonuniform, i.e., are characterized by a large field gradient ∇H. The gradient of the field, along with its strength, represents an important physical characteristic of a magnetic field, since it exerts a force effect on various physical objects. For example, the field gradient determines the effect of a magnetic field on biological systems. As a measure of the action of a magnetic field on such structures, the product $H\nabla H$ gained widespread acceptance [74]. Like the strength of the strong magnetic field, the gradient should have limiting values because of the finite values of other physical parameters. In Ref. [75], the limiting values of the field gradient were determined, and its related mechanical stresses were estimated.

7.1 Gradient of strong stray fields in a system A

The authors of Ref. [75], when analyzing the gradient of a strong stray field, considered a system of two magnets (system A) (see Fig. 3), whose stray field strength is characterized by two dependences (6) and (7) for the $H_x(x,z)$ and $H_z(x,z)$ components. Since as $b \to \infty$ the stray field is found to be two-dimensional, the tensor of the field gradient is characterized by four quantities. The components of the tensor of the field gradient are determined from the condition $\mathrm{d}\mathbf{H} = T_H\,\mathrm{d}\mathbf{r}$, where

$$T_H = \begin{vmatrix} \dfrac{\partial H_x}{\partial x} & \dfrac{\partial H_z}{\partial x} \\ \dfrac{\partial H_x}{\partial z} & \dfrac{\partial H_z}{\partial z} \end{vmatrix} . \tag{19}$$

Since the magnetic field H is a potential field [76], the tensor T_H of the field gradient is symmetrical, and the following conditions are fulfilled for its components:

$$\frac{\partial H_z}{\partial z} = -\frac{\partial H_x}{\partial x}\,, \qquad \frac{\partial H_z}{\partial x} = \frac{\partial H_x}{\partial z}\,. \tag{20}$$

Using formulas (6) and (7) for the system of two magnets, the following expressions were found for the components of the tensor of the field gradient:

$$\begin{aligned} \frac{\partial H_x(x,z)}{\partial x} &= 4M_{\mathrm{s}}\,\frac{x}{x^2+z^2} - 2M_{\mathrm{s}}\,\frac{a+x}{(a+x)^2+z^2} \\ &\quad - 2M_{\mathrm{s}}\,\frac{x-a}{(a-x)^2+z^2}\,, \\ \frac{\partial H_x(x,z)}{\partial z} &= 4M_{\mathrm{s}}\,\frac{z}{x^2+z^2} - 2M_{\mathrm{s}}\,\frac{z}{(a+x)^2+z^2} \\ &\quad - 2M_{\mathrm{s}}\,\frac{z}{(x-a)^2+z^2}\,, \\ \frac{\partial H_z(x,z)}{\partial z} &= -4M_{\mathrm{s}}\,\frac{x}{x^2+z^2} + 2M_{\mathrm{s}}\,\frac{a+x}{(a+x)^2+z^2} \\ &\quad + 2M_{\mathrm{s}}\,\frac{x-a}{(x-a)^2+z^2}\,, \\ \frac{\partial H_z(x,z)}{\partial x} &= 4M_{\mathrm{s}}\,\frac{z}{x^2+z^2} - 2M_{\mathrm{s}}\,\frac{z}{(a+x)^2+z^2} \\ &\quad - 2M_{\mathrm{s}}\,\frac{z}{(x-a)^2+z^2}\,, \end{aligned} \tag{21}$$

where a is the characteristic dimension of the magnets.

It follows from Eqn (21) that, in the points lying on the surface of the magnets ($z = 0$) with the coordinates $x = \pm a$ and $x = 0$, all the components of the tensor of the field gradient tend to infinity. These points are also singular for both the component H_x of the stray field of the system A magnets and for the components of the tensor of the gradient, i.e., the gradient of the field reaches its highest values at the same points as the field H_x does.

If the components of the tensor of the field gradient are known, we can calculate $\nabla_{\mathbf{n}} H$ — the derivative of the vector of the field with respect to the direction $\mathbf{n}$. Thus, for an arbitrary direction $\mathbf{n} = \mathbf{i}\cos\varphi + \mathbf{k}\sin\varphi$, this vector will hold the relationship $\nabla_{\mathbf{n}} H = T_H\,\mathbf{n}$. If we substitute the values of the tensor components from Eqn (21) into the last formula, then at small distances from the y-axis, $r = (x^2+z^2)^{1/2} \ll a$, we will come to the conclusion that the quantity $|\nabla_{\mathbf{n}} H|$ is independent of the direction of the vector $\mathbf{n}$ drawn from the origin (point O):

$$|\nabla_{\mathbf{n}} H| \approx 4M_{\mathrm{s}}\,\frac{\sqrt{2}}{(x^2+z^2)^{1/2}} \approx 4M_{\mathrm{s}}\,\frac{\sqrt{2}}{r}\,. \tag{22}$$

It follows from formula (22) that the magnitude of the gradient is independent of the characteristic dimension a of the magnet. This is valid when $r \ll a$. If $r > 0.01a$, expression (21) should be used for the calculation of the gradient.

Analogous dependences for the field gradient in other systems studied can be found from the limiting dependences of the strong field strength for these systems. For example, the gradient of the field above one magnet in the form of a parallelepiped will be two times smaller than what follows from dependence (22), resulting in $\nabla H \approx 2M_{\mathrm{s}}(1/r)$. For open systems consisting of three or four magnets, similar calculations give $\nabla H \approx 3\sqrt{3}M_{\mathrm{s}}(1/r)$ and $\nabla H \approx 4\sqrt{2}M_{\mathrm{s}}(1/r)$, respectively. In the above-considered systems consisting of a greater number of magnets, the strong stray field strength is described by the relation $H \approx A(n)M_{\mathrm{s}}\ln(a/r)$ for $r \ll a$. It seems likely that the approximate formula $\nabla H \approx A(n)M_{\mathrm{s}}(1/r)$ can be used for estimating the upper values of the field gradient in such systems.

By using formula (22), we can estimate the limiting achievable values of the field gradient for a system A. It is seen from this formula that the gradient of the stray field in a small region in the vicinity of a singular point can reach high values, such as $\nabla H = 10^6 - 10^8$ Oe cm^{-1} at $r \approx 0.5 - 100$ μm and a sufficiently large characteristic dimension of the magnet a ($r < 0.01a$). It is worth noting that the given dependences are applicable only for an approximate estimation of the limiting values of the gradient. In actual systems of magnets, the field gradient will be lower.

It should be emphasized that the large values of the gradient can be obtained not only with the use of magnets possessing a giant magnetic anisotropy. For example, a high-gradient magnetic field arises at the edge of a parallelepiped (made of a material with large M_{s}) placed in a strong magnetic field with a strength of several hundred kilooersteds [33]. Even higher values of the gradient can be reached in a narrow gap between conical pole pieces that are in a strong magnetic field generated by a superconducting magnet [72, 74]. In a strong field, the pole pieces will be uniformly magnetized; consequently, the magnitude of the gradient can be estimated for such a system by the formula $\nabla H \approx 4.8M_{\mathrm{s}}(1/r)$. Since the magnetization of the material of a conical pole piece can exceed the M_{s} value of the material of the magnets twofold, the field gradient in such a system will be the highest. However, the field gradient in an optimized quasinonuniform system of eight magnets can be the same, or even greater. This is seen from the limiting dependence $\nabla H \approx 8\sqrt{2}M_{\mathrm{s}}(1/r)$ for the field gradient. Magnetic fields with an even higher gradient can be produced in systems of magnets which generate point stray fields. To this end, permanent magnets with a large saturation induction and giant magnetic anisotropy should be used, e.g., those made of $SmCo_5$ ($H_K \approx 450$ kOe) [77]. In this case, the magnitude of the magnetic field gradient at small distances from the edge of the magnet can reach $\nabla H \approx 10^7$ Oe cm^{-1}.

7.2 Mechanical stresses in systems of magnets generating strong stray fields

As is seen, a distinctive feature of strong stray fields of magnets with a giant magnetic anisotropy is the existence of singularities both in the values of fluctuating field strength and of its gradient. Since the field gradient near singular points takes on very large values, it is of interest to determine the possible values of mechanical stresses. It is known [78] that internal stresses arise due to the action of ponderomotive forces in a ferromagnet located in an external uniform magnetic field H. The magnitude of the mechanical stresses is proportional to $H^2/8\pi$, and at the external field strength $H \sim 10^4$ Oe comes to $\sigma \sim 0.05$ kgf mm^{-2}. If the magnetic field is nonuniform, additional stresses related to the field gradient can arise. The authors of Ref. [75] estimated them for a system A.

The force acting in a permanent magnet on an elementary region of the magnet with a volume ΔV magnetized to saturation is written out as

$$\Delta\mathbf{F}(x,z) = T_H\mathbf{M} = T_H\mathbf{M}_{\mathrm{s}}\,\Delta V. \tag{23}$$

Consequently, the expression for the specific force is as follows: $\mathbf{f}(x,z) = \Delta\mathbf{F}(x,z)/\Delta V = T_H\mathbf{M}_{\mathrm{s}}$ or $\mathbf{f} = \boldsymbol{\nabla}(\mathbf{M}_{\mathrm{s}}\mathbf{H}) = (\mathbf{M}_{\mathrm{s}}\boldsymbol{\nabla})\mathbf{H}$, where $\boldsymbol{\nabla} = (\partial/\partial x)\mathbf{i} + (\partial/\partial z)\mathbf{k}$, and $\mathbf{i}$ and $\mathbf{k}$ are the unit vectors.

In a system of two type A magnets, the magnetization vector at all the points of the magnet is directed parallel to the z-axis; consequently, $\mathbf{M}_z = M_{\mathrm{s}}\mathbf{k}$. Taking this into account, the expression (23) for the specific force takes on the form

$$\mathbf{f}(x,z) = M_z\,\frac{\partial H_z}{\partial x}\,\mathbf{i} + M_z\,\frac{\partial H_z}{\partial z}\,\mathbf{k} = M_z\,\frac{\partial H_x}{\partial z}\,\mathbf{i} + M_z\,\frac{\partial H_z}{\partial z}\,\mathbf{k}\,. \tag{24}$$

It follows from the last expression that the force $\mathbf{f}$ is resolved into two components: f_x and f_z. One of these components causes a compression of the magnet, while the other causes its tension. If we substitute into formula (24) the expressions for the components (21) of the tensor of the field gradient, we obtain the absolute value of the specific force (density of the force):

$$\begin{aligned}\left|\mathbf{f}(x,z)\right| &\approx M_z\left[\left(\frac{\partial H_x}{\partial z}\right)^2 + \left(\frac{\partial H_z}{\partial z}\right)^2\right]^{1/2} \\ &\approx 4M_{\mathrm{s}}^2\,\frac{1}{(x^2+z^2)^{1/2}} \approx \frac{4M_{\mathrm{s}}^2}{r}\,.\end{aligned} \tag{25}$$

Expression (25) describes the density of volume forces at small r ($r \ll a$). For $r > 0.1a$, $\mathbf{f}(x,z)$ should be calculated using exact expressions for the components (21) of the tensor of the field gradient.

It follows from expression (25) that the volume force density tends to infinity as $r \to 0$. However, $f(x,z)$ will be finite, since the minimum distance from the edge of the magnet cannot be less than about $10^{-7}-10^{-8}$ cm, i.e. $r \geqslant 10^{-7}-10^{-8}$ cm. Notice that even at a macroscopic distance $r = 1$ μm, the volume force density remains very high: $f(x,z) \approx 5\times10^{10}$ dyn cm^{-3}. This value of the density, for example, exceeds the density of the gravity force $f = g\rho$ (where g is the acceleration of gravity, and ρ is the density of the material of the magnet) by a factor of $\sim 10^7$.

As is seen, a distinctive feature of the systems of magnets generating strong stray fields is the high density of volume forces localized near singular points of the strong magnetic field. These forces lead to the appearance of mechanical stresses in the magnet. Since the calculation of the stressed state caused by the stray field in a magnet is a complex problem of the theory of elasticity, the authors of Ref. [75] only estimated the magnitude of stresses in a thin subsurface layer that is not coupled elastically with the magnet, i.e., in a thin film on the magnet. Thus, in a thin layer of thickness Δx and of area ΔS adjacent to the edge of the magnet (with coordinates $z \approx 0$, $r = x \approx \Delta x \approx 10^{-7}$ cm), the stress is given by

$$\sigma_{\mathrm{edge}} = f\,\frac{\Delta V}{\Delta S} = f\Delta x \approx A(n)M_{\mathrm{s}}^2\,\frac{\Delta x}{x}\,. \tag{26}$$

Since the distance $r = x \approx \Delta x$ at the edge of the magnet, so then $\sigma_{\mathrm{edge}} \approx A(n)M_{\mathrm{s}}^2\Delta x/\Delta x = A(n)M_{\mathrm{s}}^2$. If we assume $M_{\mathrm{s}} = 1000$ G and $A(n) = 10$, then we obtain $\sigma_{\mathrm{edge}} \approx 10^7$ dyn cm^{-2} ≈ 0.1 kgf mm^{-2}. As is seen from these calculations, the stresses near the singular point ($x = 0$, $z \approx 0$) are small and they cannot affect the values of the magnetic parameters of the material of the magnet.

For the appearance of high mechanical stresses in a magnet, the presence of a high density of volume forces at singular points of the magnet is apparently insufficient. The point is that these forces decrease rapidly when moving away from the singular points (according to a hyperbolic law); in addition, they are localized in a very small volume of the magnet. Upon moving away from the point O in a system A (increase in r or x), the force density f will decrease, but the stresses $\sigma(x)$ will strengthen.

The *limiting* magnitude of stress σ arising in the magnet was assessed. When estimating the limiting values of σ, we restricted ourselves to the calculation of stress in a thin subsurface layer of a system A, which is not coupled elastically with the magnet body. Such a system can, for example, be realized if a system A is coated by a thin ferromagnetic film. This film will be strained under the action of volume forces almost independently of the magnet, and the stress in the film will be substantially higher than those in the magnet. In the estimations, we restricted ourselves to evaluating only one component, f_x, assuming it to be equal to $f_x = A(n)M_{\mathrm{s}}^2/x$. This assumption will lead to overestimated values of stresses compared to their true values. The stress $\sigma(x)$ in such a layer, which arise in an elementary region of area $\Delta S = \Delta z\Delta y$ located on the subsurface layer of the magnet at a distance x from the y-axis in the point M$(x,0)$, can be calculated as follows: $\sigma(x) = F_x(x)/\Delta S$, where $F_x(x)$ is the horizontal component of the force applied to the elementary area ΔS:

$$F_x(x) = \int_V f(x)\,\mathrm{d}V = \int_{x_{\min}}^{x} 4M_{\mathrm{s}}^2\Delta S\,\frac{\mathrm{d}x}{x}\,, \tag{27}$$

where $x_{\min}$ is the minimum distance from the edge of the magnet, which is assumed to be equal to the interatomic spacing, namely to $10^{-7}-10^{-8}$ cm, and thus

$$\sigma(x) \approx \int_{x_{\min}}^{x} \frac{4M_{\mathrm{s}}^2}{x}\,\mathrm{d}x = 4M_{\mathrm{s}}^2\ln\frac{x}{x_{\min}}\,. \tag{28}$$

From the last formula it follows that the magnitude of stress does not exceed σ ranging approximately $1-3$ kgf mm^{-2}.

8. Application perspectives of strong stray fields

To date, only examples of practical applications of strong stray fields arising in Halbach cylinders have been known [2]. This appears to be related to the fact that information on strong fields was absent for a wide class of systems of magnets. In the examples that are given below, we unveil the potential put in the application of strong fields in the technology of magnetic recording, for the development of EPR microscopes, refrigerating devices, and separators for the separation of weakly magnetic substances, and as a tool for acting on biological subjects. These examples are original and previously unknown, which additionally emphasizes the novelty of the discovered phenomenon — *strong stray fields*. At the same time, possible areas for the practical application of strong fields can be substantially wider than in the examples described in Sections 8.1–8.4.

8.1 Application of strong fields in the technology of magnetic recording. Physical foundations of the method

The main problems in the technology of magnetic recording from the very moment of its appearance are an increase in the density of information recorded on the carrier and an increase in the reliability of its storage. In the last decade, the density of recording on hard disks has increased by a factor of 1000, and the size of an imprint on the carrier has decreased to $d \approx 15$ nm. A further increase in the density of recording is restricted by the so-called superparamagnetic limit [79]. The authors of Refs [80, 81] and of the patent [82] see the possibility of employing highly coercive carriers based on materials with a giant magnetic anisotropy as one of the ways to solve this problem. The superparamagnetic limit can be reduced to $d \approx 2$ nm by using carriers with a magnetic anisotropy constant $K \approx 5 \times 10^7 - 10^8$ erg cm^{-3}. This refers to both planar and perpendicular types of recording, as well as to recording with the use of vortex structures [83, 84]. The information recorded on highly coercive carriers will be weakly sensitive to the effect of random magnetic fields, i.e., the reliability of its storage will increase. This is especially important for archiving various documents.

At present, the employment of highly coercive carriers in the technology of magnetic recording encounters obstacles because of the absence of recording heads capable of locally magnetizing such highly coercive media with $H_c > 5$ kOe. Figure 14a demonstrates a schematic diagram of a head for horizontal recording. The head consists of two magnets having mutually opposite directions of magnetization, and a system for generating a magnetic biasing field. The pair of film magnets is analogous to a system A. The biasing system consists of magnetically soft layers and a winding.

The recording is implemented as follows. The head is placed above the carrier at such a distance t that the horizontal component of the stray field produced by the magnets is somewhat less than the coercive force H_c of the carrier. Then, the biasing system is switched on, which creates an additional pulsed field ΔH of such a strength whereat the resulting field $\Delta H + H_x$ becomes greater than the coercive force H_c of the carrier. The fact that the field H_x can be strong is seen from Figure 14b.

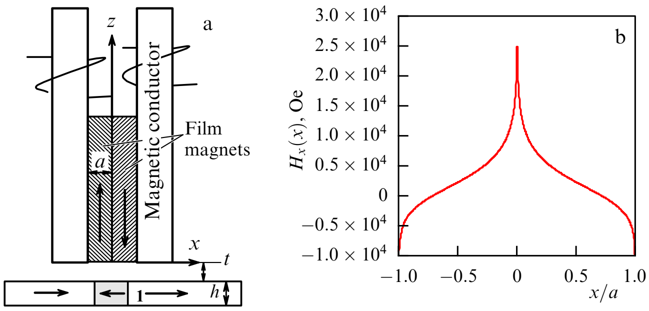

Figure 14. (a) Schematic of a head for horizontal recording. (b) Strength of the horizontal component $H_x(x)$ of the stray field constructed for points falling in the range $-a < x < a$ on the plane xy ($z = 0.01a$, $y = 0$). It was assumed in the calculations that the dimension of the magnets in the direction of the y-axis is $b = 2a$, and $M_s = 1000$ G.

The size of the imprint depends on the size a of the magnets, the coercive force H_c, the biasing field ΔH, the distance t from the carrier to the head, and the saturation magnetization of the material of the magnets for the head. By varying these parameters, one can optimize the recording process. Thus, to obtain an imprint of small dimensions ($\Delta x < 0.1$ μm), carriers with a large coercive force ($H_c \gtrsim 5000$ Oe) should be used.

Since the magnets of the heads for dense recording should be thin film, one of the key moments for the realization of recording on highly coercive carriers is the production of such film layers. Similar films are necessary for both the heads and the carriers. Investigations performed in recent years show the possibility of producing such highly coercive film layers. Thus, the authors of Refs [27, 85] describe the technology of obtaining films from Co–Pt and Fe–Pt alloys with a coercive force $H_c \sim 50$ kOe.

Schematic diagram of one of the possible variants of the head for vertical recording differs only a little from the appropriate diagram showing the head for horizontal recording. The distinction lies in the fact that, in this case, the field component normal to the carrier rather than the tangential component should have high values. This is realized through harnessing the magnetization that has mutually opposite directions in the magnets. Such a system of magnets will be stable and will not be demagnetized if the coercive force of the magnets is $H_c > 4\pi M_s$. The requirements for the anisotropy field of the material of the magnets are the same as those for the horizontal head.

8.2 Application of strong stray fields for the magnetizing system of an EPR microscope

At present, EPR spectrometers. in which the dc magnetic field is uniform and magnetizes the entire object under study, are widely used in science and engineering. But sometimes a need arises to determine the physical and physicochemical properties of a sample in its local regions rather than over its entire body. Attempts to localize the action of a microwave field using a diaphragm in a metallic screen can hardly be assumed to be promising, the more so as the mass of the magnetizing system in existing EPR spectrometers varies from several hundred to a thousand kilograms. This closes the way to further miniaturization of the device.

In Refs [60, 61, 86], an operative prototype of a new EPR microscope with moderate dimensions (about $7 \times 10 \times 20$ cm) working in a millimeter wave range has been described. The working scheme of this microscope is given in Fig. 15. This microscope has noticeable advantages due to the application of a new source of magnetic field which generates a static magnetic field of a desired strength in a local region via the use of the system A magnets.

When designing a system of magnets for an EPR microscope, an important characteristic, apart from the field strength, is the minimum size of the region of the substance to be studied in which the resonant absorption occurs. It can be assumed that the volume of this region is proportional to the area of a surface of equal strength, since the resonant

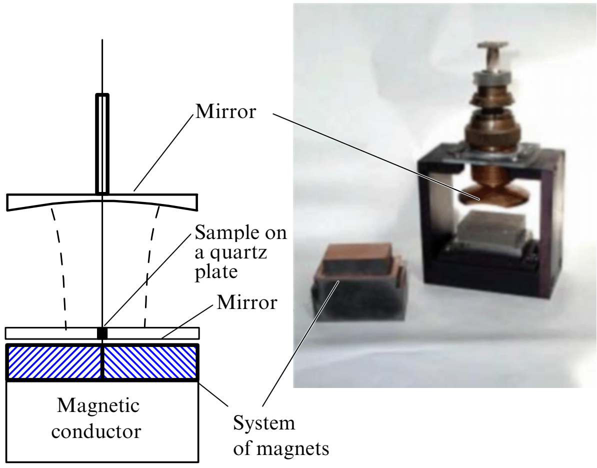

Figure 15. EPR spectrometer with a magnetizing system consisting of two permanent magnets.

absorption occurs in one–two atomic layers of the substance studied [61]. Therefore, when analyzing systems of magnets for an EPR microscope, the possible area of a surface of equal strength should also be determined, apart from the magnetic field strength.

Since about 10^6-10^7 atoms fall over an area of 1 μm^2, so the signal of the EPR spectrometer for an area of equal strength measuring $S = 10^3$ μm^2 does correspond to the signal from $\sim 10^{10}$ atoms. By recognizing that the sensitivity limit of an EPR spectrometer amounts to 10^7 atoms, we can believe that the possibility of the detection of small regions will be sufficiently high. Based on the estimates made, it can be assumed that the use of EPR microscopy will permit the detection of particles a few microns in size.

Since the sensitivity of an EPR spectrometer increases with increasing frequency, to heighten the sensitivity requires the employment of sources with stronger stray fields than those existing in the above-considered system A. This can be realized in systems that consist of a large number of magnets, e.g., in quasinonuniform systems. The first experiments with the new EPR microscope that were performed in the millimeter wave range demonstrated a significant potential of this device and the possibility of its application for the investigation of micro- and nanostructured materials and objects. The small dimensions of the magnetizing system built around permanent magnets and of the very EPR microscope offer considerable scope for its application in industrial and field conditions.

8.3 Application perspectives of strong stray fields in refrigerating devices

In Ref. [87], we substantiated the possibility of using systems of magnets that generate strong stray fields in refrigerating equipment on the basis of materials with a giant magnetocaloric effect. It has been shown that for these purposes the most suitable systems are those consisting of cylindrical magnets with a radial magnetization or quasinonuniform systems generating stray fields with a large region of localization of the strong field. To quantitatively estimate various such systems, a special parameter — specific field H_{SF} — has been introduced:

$$H_{SF} = \frac{1}{V_w + V_m} \int_{V_w+V_m} H(x,y,z)\,dV\,, \tag{29}$$

where V_m is the volume of the magnets, and V_w is the volume of the working space.

It has been shown that, when utilizing quasinonuniform systems and cylindrical magnets with a radial magnetization, the specific field can reach values such as $H_{SF} \approx 5M_s$. This value of the specific field is greater compared with the system of magnets in the Halbach cylinder that was used for the refrigerating equipment in Ref. [79].

8.4 Application of strong stray fields for the separation of weakly magnetic substances

The existence of high-gradient magnetic fields near singular points in systems of permanent magnets with large anisotropy makes it possible to utilize such systems in magnetic separators for separating substances with a small magnetic susceptibility χ. These can also be paramagnets with $\chi > 10^{-4}$.

At present, ferrite magnets found use for the beneficiation of magnetite ores in magnetic separators. The stray fields produced by such magnets are sufficient for the separation of magnetite (Fe_3O_4) from dead rock. However, these fields prove to be insufficient for the separation of hematite ores. The point is that hematite (Fe_2O_3) with a rhombohedral crystal lattice relates to weak ferromagnets having a rather small magnetization: $M_s \sim 0.5$ G [16]. To hold hematite particles on a cylindrical surface of a drum type separator, a sufficiently large magnetic field with a high gradient is necessary. The magnitude of the necessary holding force can be estimated as $F \approx M_s \,\mathrm{grad}\, H$. The calculation shows that the attraction force F will exceed the weight of a hematite particle if the field gradient is $\mathrm{grad}\, H \geqslant 5000$ Oe cm^{-1}, and the magnetization is $M \sim 1$ G. As is seen, the field in the separator for the beneficiation of hematite ores should be not only high-gradient but also sufficient for the magnetization of the Fe_2O_3 particles to saturation. Such a field can be generated by a simple system comprising two type A magnets.

9. Conclusions

The main above-considered results can be formulated as follows:

(1) Using the solutions to magnetostatic problems as the examples, the existence of strong stray magnetic fields in various systems of magnets has been substantiated and conditions for their appearance have been determined. It has been shown that a necessary condition for their appearance is a large field of uniaxial anisotropy H_K of the material of the magnet, substantially exceeding its saturation induction: $H_K \gg 4\pi M_s$.

(2) The existence of strong stray magnetic fields has been proved by direct measurements with the aid of magnetoresistive sensors and EPR spectrometry. It has been shown that the measured values of the field agree well with the calculated logarithmic dependence $H \approx 4M_s \ln(r/a)$.

(3) A classification of strong magnetic fields that can be produced by various systems of permanent magnets has been performed. Depending on the shape of the region of the field localization, three types of strong fields have been defined: *linear, point, and uniform strong fields*. The limiting values of the stray field have been calculated for fields of each type. It has been shown that the limiting value of a linear field cannot be higher than that following from the dependence $H \approx 4\pi M_s \ln(r/a)$. The results obtained by the authors of this paper indicate the possibility of achieving stray fields with

an induction $B \approx 10$ T in materials with giant magnetic anisotropy.

(4) It has been found that the magnitude of the field gradient can reach values of about $|\nabla H| \approx 10^6 - 10^8$ Oe cm^{-1} in the systems of magnets with giant magnetic anisotropy. This magnitude of the field gradient is comparable with the value obtained for a high-gradient stray field in superconducting magnets with conical pole pieces made of materials with a high induction.

(5) Strong high-gradient magnetic fields constitute a new, little-investigated factor to act on various physical objects and biological systems. Examples of the application of strong fields in various original devices have been demonstrated.

Acknowledgments
We are deeply grateful to V G Bar'yakhtar and Yu I Gorobets for fruitful discussions of the results given in the paper, and for perceptive remarks.

References

1. Halbach K *Nucl. Instrum. Meth.* **169** 1 (1980)
2. Halbach K *J. Appl. Phys.* **57** 3605 (1985)
3. Leupold H A, Potenziani E *J. Appl. Phys.* **63** 3987 (1988)
4. Leupold H A, Potenziani E *J. Appl. Phys.* **70** 6621 (1991)
5. Leupold H A, Tilak A S, Potenziani E *J. Appl. Phys.* **76** 6859 (1994)
6. Leupold H A, McLane G F *J. Appl. Phys.* **76** 6253 (1994)
7. Bloch F et al. *Eur. Phys. J. Appl. Phys.* **5** 85 (1999)
8. Zhu Z Q et al. *IEEE Trans. Magn.* **36** 3349 (2000)
9. Naoyuki I, in *China Magnet Symp., May 17–21, 2004, Xi'an, China* (X'ian: Shanghamag Inform. Consulting Co., 2004) p. 103
10. Samofalov V N et al., in *Novye Magnitnye Materialy Mikroelektroniki. Sb. Trudov XVIII Mezhdunar. Shkoly-Seminara, 24–28 Iyunya 2002 g., Moskva* (New Magnetic Materials of Microelectronics. Collection of Papers of the 18th Intern. School-Seminar, June 24–28, 2002, Moscow) (Moscow: Izd. MGU, 2002) p. 366
11. Samofalov V N et al. *J. Magn. Magn. Mater.* **281** 326 (2004)
12. Samofalov V N et al. *Phys. Met. Metallogr.* **97** 235 (2004) [*Fiz. Met. Metalloved.* **97** (3) 15 (2004)]
13. Bozorth R M *Ferromagnetism* (New York: Van Nostrand, 1951) [Translated into Russian: (Moscow: IL, 1956)]
14. Vonsovskii S V, Shur Ya S *Ferromagnetizm* (Ferromagnetism) (Moscow: Gostekhizdat, 1948)
15. Chikasumi S *Physics of Ferromagnetism: Magnetic Characteristics and Engineering Application* (Tokyo: Syokabo, 1984) [Translated into Russian (Moscow: Mir, 1987)]
16. Chikasumi S *Physics of Ferromagnetism: Magnetic Properties of Matter* (Tokyo: Syokabo, 1980) [Translated into Russian (Moscow: Mir, 1983)]
17. Nesbitt E A, Wernick J H *Rare Earth Permanent Magnets* (New York: Academic Press, 1973) [Translated into Russian (Moscow: Mir, 1977)]
18. Belov K P *Redkozemel'nye Magnetiki i Ikh Primenenie* (Rare-Earth Magnets and Their Application) (Moscow: Nauka, 1980)
19. Jiles D C *Acta Mater.* **51** 5907 (2003)
20. Mishin D D *Magnitnye Materialy* (Magnetic Materials) (Moscow: Vysshaya Shkola, 1991)
21. Nikitin S A *Magnitnye Svoistva Redkozemel'nykh Metallov i Ikh Splavov* (Magnetic Properties of Rare-Earth Metals and Their Alloys) (Moscow: Izd. Mosk. Univ., 1989)
22. Coey J M D *J. Alloys Comp.* **326** 2 (2001)
23. Skomski R, Sellmyer D J *J. Rare Earths* **27** 675 (2009)
24. Skomski R, Sellmyer D J, in *Handbook of Advanced Magnetic Materials* (Eds Y Liu, D J Sellmyer, D Shindo) Vol. 1 (New York: Springer, 2006) p. 1
25. Buschow K H J, in *Handbook of Magnetic Materials* Vol. 10 (Ed. K H J Buschow) (Amsterdam: Elsevier, 1997) p. 463
26. *2000 China Magnet Symp.* (X'ian: Shanghamag Inform. Consulting Co., 2000) p. 207
27. Shafer R et al., in *China Magnet Symp., May 17–21, 2004, Xi'an, China* (Xi'an: Shanghaimag Inform. Consulting Co., 2004) p. 363
28. Malozemoff A P, Slonczewski J C *Magnetic Domain Walls in Bubble Materials* (New York: Academic Press, 1979) [Translated into Russian (Moscow: Mir, 1982)]
29. Elliott R J *Phys. Rev.* **124** 346 (1961)
30. Irkhin Yu P *Sov. Phys. JETP* **23** 253 (1966) [*Zh. Eksp. Teor. Fiz.* **50** 379 (1966)]
31. Irkhin Yu P *JETP Lett.* **12** 28 (1970) [*Pis'ma Zh. Eksp. Teor. Fiz.* **12** 38 (1970)]
32. Mushnikov N V *Phys. Usp.* **55** 421 (2012) [*Usp. Fiz. Nauk* **182** 450 (2012)]
33. Joseph R I, Schlömann E *J. Appl. Phys.* **36** 1579 (1965)
34. Thiaville A, Tomáš D, Miltat J *Phys. Status Solidi A* **170** 125 (1998)
35. Rave W, Ramstöck K, Hubert A *J. Magn. Magn. Mater.* **183** 329 (1998)
36. Shtrikman S, Treves D *J. Appl. Phys.* **31** S72 (1960)
37. Kittel Ch, in *Fizika Ferromagnitnykh Oblastei* (Physics of Ferromagnetic Domains) (Ed. S V Vonsovskii) (Moscow: IL, 1951) p. 19
38. Kittel C *Rev. Mod. Phys.* **21** 541 (1949)
39. Landau L D, Lifshitz E M *Electrodynamics of Continuous Media* (Oxford: Pergamon Press, 1960) [Translated from Russian: *Elektrodinamika Sploshnykh Sred* (Moscow: Fizmatgiz, 1959)]
40. Schlömann E *J. Appl. Phys.* **44** 1837 (1973)
41. Schlömann E *J. Appl. Phys.* **44** 1850 (1973)
42. Slonczewski J C *J. Appl. Phys.* **44** 1759 (1973)
43. Mal'ginova S D et al., in *Novye Magnitnye Materialy Mikroelektroniki. Sb. Trudov XIX Mezhdunar. Shkoly-Seminara, 28 Iyunya–2 Iyulya 2004 g., Moskva* (New Magnetic Materials of Microelectronics. Collection of Papers of the 19th Intern. School-Seminar, June 28–July 2, 2004, Moscow) (Moscow: Izd. Fiz. Fakul'teta MGU, 2004) p. 804
44. Mal'ginova S D et al. *Phys. Met. Metallogr.* **103** 348 (2007) [*Fiz. Met. Metalloved.* **103** 364 (2007)]
45. Bilenskii V P *Sov. Phys. Tech. Phys.* **18** 527 (1973) [*Zh. Tekh. Fiz.* **43** 840 (1973)]
46. Mitsek A I, Semyannikov S S *Fiz. Met. Metalloved.* **35** 1163 (1973)
47. Filippov B N, Lebedev Yu G, Onoprienko L G *Fiz. Met. Metalloved.* **38** 702 (1974)
48. Kaczér J, Murtinová L *Phys. Status Solidi A* **23** 79 (1974)
49. Jakubovics J P *Philos. Mag.* **14** 881 (1966)
50. Antonov L I et al., in *Novye Magnitnye Materialy Mikroelektroniki. Sb. Trudov XVIII Mezhdunar. Shkoly-Seminara, 24–28 Iyunya 2002 g., Moskva* (New Magnetic Materials of Microelectronics. Collection of Papers of the 18th Intern. School-Seminar, June 24–28, 2002, Moscow) (Moscow: Izd. MGU, 2002) p. 402
51. Antonov L I, Mukhina E A, Lukasheva E V *Phys. Met. Metallogr.* **78** 357 (1994) [*Fiz. Met. Metalloved.* **78** (4) 5 (1994)]
52. Ivoilov N G et al. *Fiz. Met. Metalloved.* **64** 1196 (1987)
53. Palatnik L S, Ravlik A G, Samofalov V N *Fiz. Tverd. Tela* **20** 428 (1978)
54. Palatnik L S, Ravlik A G, Samofalov V N *Fiz. Tverd. Tela* **19** 830 (1977)
55. Palatnik L S et al. *Fiz. Met. Metalloved.* **47** 954 (1979)
56. Palatnik L S et al. *Fiz. Tverd. Tela* **23** 3706 (1982)
57. Akhiezer A I, Bar'yakhtar V G, Peletminskii S V *Spin Waves* (Amsterdam: North-Holland, 1968) [Translated from Russian: *Spinovye Volny* (Moscow: Nauka, 1967)]
58. Lisovskii F V, Antonov L I (Eds) *Magnetizm i Magnitnye Materialy: Terminologicheskii Spravochnik* (Magnetism and Magnetic Materials: A Handbook of Terms) (Moscow: Vagrius, 1997)
59. Avramenko B A et al., in *Novye Magnitnye Materialy Mikroelektroniki. Sb. Trudov XVIII Mezhdunar. Shkoly-Seminara, 24–28 Iyunya 2002 g., Moskva* (New Magnetic Materials of Microelectronics. Collection of Papers of the 18th Intern. School-Seminar, June 24–28, 2002, Moscow) (Moscow: Izd. MGU, 2002) p. 282
60. Tarapov S I et al. *Int. J. Infrared Millimeter Waves* **24** 1081 (2003)
61. Belozorov D et al. *Int. J. Infrared Millimeter Waves* **27** 105 (2006)
62. Il'yashenko E I, Lubyanyi L Z, Samofalov V N *Instrum. Exp. Tech.* **48** 503 (2005) [*Prib. Tekh. Eksp.* (4) 89 (2005)]
63. Samofalov V N, Belozorov D P, Ravlik A G *Phys. Met. Metallogr.* **102** 494 (2006) [*Fiz. Met. Metalloved.* **102** 527 (2006)]
64. Samofalov V N, Doctoral Dissertation (Phys.-Math.) (Kharkov: Karazin National Univ., 2009)

65. Zhakov S V *Phys. Met. Metallogr.* **96** 562 (2003) [*Fiz. Met. Metalloved.* **96** (6) 18 (2003)]
66. Belozorov D, Ravlik A, Samofalov V *J. Iron Steel Res. Int.* **13** (Suppl. 1) 483 (2006)
67. Elsgolts L *Differential Equations and the Calculus of Variations* (Moscow: Mir Publ., 1970) [Translated from Russian: *Differentsial'nye Uravneniya i Variatsionnoe Ischislenie* (Moscow: Nauka, 1965)]
68. Samofalov V N, Belozorov D P, Ravlik A G *J. Magn. Magn. Mater.* **320** 1490 (2008)
69. Samofalov V N, Belozorov D P, Ravlik A G *Phys. Met. Metallogr.* **107** 133 (2009) [*Fiz. Met. Metalloved.* **107** 144 (2009)]
70. Zhang B, Hatch G P *IEEE Trans. Magn.* **45** 4395 (2009)
71. Montgomery D B, in *Proc. of the Intern. Conf. on High Magnetic Fields, 1961* (Cambridge: MIT Press, 1962) p. 180
72. Nikitin S A et al. *Prib. Tekh. Eksp.* (2) 201 (1977)
73. Bulatov A S *Vopr. At. Nauki Tekh.* (4) 20 (2006)
74. Maret G, Dransfeld K, in *Strong and Ultrastrong Magnetic Fields and Their Applications* (Topics in Applied Physics, Vol. 57, Ed. F Herlach) (Berlin: Springer-Verlag, 1985) p. 80 [Translated into Russian (Moscow: Mir, 1988) p. 180]
75. Samofalov V N, Belozorov D P, Ravlik A G *Funct. Mater.* **15** 407 (2008)
76. Vonsovskii S V *Magnetism* (New York: J. Wiley, 1974) [Translated from Russian: *Magnetizm* (Moscow: Nauka, 1971)]
77. Ermolenko A S, Korolev A V *JETP Lett.* **21** 15 (1975) [*Pis'ma Zh. Eksp. Teor. Fiz.* **21** 34 (1975)]
78. Tamm I E *Fundamentals of the Theory of Electricity* (Moscow: Mir Publ., 1979) [Translated from Russian: *Osnovy Teorii Elektrichestva* (Moscow: Nauka, 1966)]
79. Brown W F (Jr.) *Phys. Rev.* **130** 1677 (1963)
80. Samofalov V N et al. *J. Optoelectron. Adv. Mater.* **6** 911 (2004)
81. Samofalov V N et al., in *Proc. of the 4th Intern. Workshop on Materials for Electrical Engineering, Bucharest, Romania, May 26–28, 2004*, p. 43
82. Samofalov V N et al., US Patent 7,492,550, Filed November 18, 2003 (2009)
83. Kravchuk V P, Sheka D D *Phys. Solid State* **49** 1923 (2007) [*Fiz. Tverd. Tela* **49** 1834 (2007)]
84. Stanciu C D et al. *Phys. Rev. Lett.* **99** 047601 (2007)
85. Rozman K Z et al. *IEEE Trans. Magn.* **45** 4413 (2009)
86. Belozorov D P et al., in *Novye Magnitnye Materialy Mikroelektroniki. Sb. Trudov XX Mezhdunar. Shkoly-Seminara, Moskva* (New Magnetic Materials of Microelectronics. Collection of papers of the 20th Intern. School-Seminar, Moscow) (Moscow: Izd. MGU, 2006) p. 671
87. Belozorov D P et al. *Metallofiz. Noveishie Tekhnol.* **32** 1591 (2010)